The role of root community attributes in predicting soil fungal and bacterial community patterns

Jesús López-Angulo (ORCID ID: 0000-0003-3539-2545)[1], Marcelino de la Cruz (0000-0002-9080-4525)[1], Julia Chacón-Labella (0000-0002-6787-1295)[2], Angela Illuminati (0000-0003-2313-1639)[1], Silvia Matesanz (0000-0003-0060-6136)[1], David S. Pescador (0000-0003-0395-9543)[1], Beatriz Pías (0000-0002-1136-8914)[3], Ana M. Sánchez ()[1] and Adrián Escudero (0000-0002-1427-5465)[1]

[1] Área de Biodiversidad y Conservación. Universidad Rey Juan Carlos, 28933, Móstoles, Madrid, Spain;

[2] Department of Ecology and Evolutionary Biology, University of Arizona, Tucson, AZ 85721, USA;

[3] Departamento de Biodiversidad, Ecología y Evolución, Universidad Complutense de Madrid, 28040, Madrid, Spain.

Author for correspondence:

Jesús López-Angulo

Tel: +34 91488851

E-mail: jesus.lopez.angulo@urjc.es

Number of words in main text: 6523; Number of words in abstract: 199; Number of words in introduction: 1394; Number of words in methods 2667; Number of words in results 779; Number of words in discussion 1686; Number of figures which should be published in colour: 4; Number of tables: 2; Number of Appendices in supporting information: 16.

Summary

- Roots are assumed to play a major role in structuring soil microbial communities, but most studies exploring the relationships between microbes and plants at the community-level have only used aboveground plant distribution as a proxy. However, a decoupling between below- and aboveground plant components may occur due to differential spreading of plant canopies and root systems. Thus, soil microbial-plant links are not completely understood.

- Using a combination of DNA metabarcoding and spatially explicit sampling at the plant neighbourhood scale, we assessed the influence of plant root community on soil bacterial and fungal diversity (species richness, composition and β-diversity) in a dry Mediterranean scrubland.

- We found that root composition and biomass, but not richness, predict unique fractions of variation in microbial richness and composition. Moreover, bacterial β-diversity was related to root β-diversity, while fungal β-diversity was related to aboveground plant β-diversity, suggesting that plants differently influence both microbial groups.

- Our study highlights the role of plant distribution both below- and aboveground, soil properties and other spatially structured factors in explaining the heterogeneity in soil microbial diversity. These results also show that incorporating data on both plant community compartments will further our understanding of the relationships between soil microbial and plant communities.

Keywords: bacterial and fungal diversity, belowground plant community, DNA metabarcoding, microbial communities, plant-soil interactions, roots, soil biodiversity

Introduction

Microorganisms living in the soil, such as bacteria and fungi, engage with plants to form complex biotic interactions, which play key roles in controlling critical ecosystem processes, including nutrient cycling, plant primary productivity and organic matter decomposition (Van Der Heijden *et al.*, 2008; Fierer *et al.*, 2013). Given the importance of soil microbial-plant feedbacks in driving ecosystem multi-functionality and services (Bardgett & Van Der Putten, 2014; Delgado-Baquerizo *et al.*, 2015), a huge research effort has been devoted to better understand the eco-evolutionary mechanisms controlling the relationships between soil microbes and plants. Direct plant-microbial links may arise from well-known mechanisms involving pathogenic or symbiotic associations such as mycorrhizal and nitrogen-fixing bacteria (Wardle *et al.*, 2004; Wubs & Bezemer, 2016). Plants also modify the soil physicochemical conditions by the release the products of photosynthesis, the litter contribution, and the uptake of ions (Wardle *et al.*, 2004; Trinder *et al.*, 2009; Millard & Singh, 2010). Previous studies have shown that the bacterial diversity in rhizospheres are different from those of bulk soils (Uroz *et al.*, 2010; Philippot *et al.*, 2013) indicating a strong heterogeneous distribution of microbial communities at a fine scale. Despite the establishment and maintenance of soil microbial-plant interactions is strongly mediated through the direct influence of the root, there is a lack of evidence on how different community attributes of the belowground plant community, including root α-diversity, β-diversity, composition and species' abundance, influence soil bacterial and fungal diversity and community composition. This knowledge gap is due to the fact that a large body of research in this field has used information from the aboveground component, such as cover structure, standing biomass or basal area, as a surrogate for plant community attributes (Prober *et al.*, 2015; Delgado-Baquerizo *et al.*, 2018; Adamczyk *et al.*, 2019; Chen *et al.*, 2019), despite substantial evidence of an aboveground-belowground decoupling in composition and structure in different plant communities (Jones *et al.*, 2011; Träger *et al.*, 2019).

A close match between below- and aboveground plant species richness may be expected at large spatial scales, such as the landscape level. However, this coupling can be blurred at fine spatial scales (i.e. in the neighbourhood of individual plants) due to differences in the spreading of plant canopies and plant root systems (Schenk & Jackson, 2002). For instance, species richness may be higher belowground than aboveground because of the ability of some herbaceous perennials with dormant meristems to persist in the absence of aboveground organs (Reintal *et al.*, 2010; Hiiesalu *et al.*, 2012). Furthermore, plants from water-limited ecosystems often show high root:shoot ratios as a consequence of the higher investment in the

belowground counterpart (Schenk & Jackson, 2002; Mokany *et al.*, 2006). This potential decoupling between aboveground and belowground plant communities identifies a clear limitation to the establishment of causal connections between soil microbial and plant communities based only on inferences from the aboveground plant component. A usual constraint hindering the consideration of root community structure into the current framework to explain soil microbial diversity is the difficulty of characterizing root communities in the field. However, recent advances in DNA metagenomics provide a powerful tool to quantify plant species diversity and biomass partition belowground (e.g. Matesanz *et al.* 2019) and, consequently, allows testing their effects on soil microbial diversity.

Although empirical evidence on root-microbial soil interactions at the community level is sparse, several mechanisms by which plants may influence soil microbial communities through roots have been described. Roots promotes soil loosening and aeration, changing the water flow in their close vicinity (Angers & Caron, 1998; Philippot *et al.*, 2013). Roots aslo affect soil microbial diversity by altering nutrient flow rates and the partitioning of soil resources via rhizodeposits such as phenolic exudates, root cells and mucilage (Vandenkoornhuyse *et al.*, 2007; Broeckling *et al.*, 2008; Haichar *et al.*, 2008; Jones *et al.*, 2009). Therefore, it might be expected that a higher root biomass (i.e. reflecting the amount of rhizodeposits) would enhance microbial diversity (Eisenhauer *et al.* 2017). Furthermore, mounting evidence suggests the existence of a host specialization, which leads to a particular microbiota associated with specific plant roots, either through the type of rhizodeposits or other chemical-morpho-physiological traits (Silver & Miya, 2001; Jones *et al.*, 2004; Haichar *et al.*, 2008; Badri & Vivanco, 2009; Kernaghan, 2013). Under a niche coexistence framework, greater richness of roots (i.e. higher rhizodeposits variety) would lead to a higher microbial richness (De Boer *et al.*, 2005; Wardle, 2006; Eisenhauer *et al.*, 2010). In addition, host-specialization would link changes in plant species composition to changes in microbial composition, that is, belowground plant β-diversity (compositional dissimilarity of roots between sites) would predict soil microbial β-diversity (Prober *et al.*, 2015). The few experimental and observational attempts to explicitly evaluate the role of root communities as microbial drivers of microbial community structure have shown a weak or even no effect of roots (Barberán *et al.*, 2015; Leff *et al.*, 2018). The difficulties also may arise due to microbial and the two compartments of plant communities (e.g. roots and aboveground parts) are structured at different spatial and temporal scales (Bardgett *et al.*, 2005). Experimental studies may be limited by the time lags in soil microbial responses to the manipulation of plant community attributes (Hedlund *et al.*, 2003);observational evidence may also be inconclusive. For instance, Barberán *et al.* (2015), studying a tropical forest, found that

that soil microbial composition was better predicted by the distribution of plant canopies than by root distributions. This was probably due to the fact that the spatial grain size used to sample plant canopies (> 2.5 meters) better represented the variation of the plant community composition compared to the used for plant root systems (6.25 cm). Consequently, further observational and experimental studies, performed at the scale of root communities (i.e. the scale where plants interact more closely) are needed in order to progress on a more comprehensive understanding of the interactions between the belowground attributes of the plant community and microbial communities.

The relationships between roots and microbial communities may not always be causal, as they can emerge as a concomitant effect of the aboveground component of plant communities or other shared soil-driven processes. The aboveground plant community attributes have been shown to explain patterns of microbial diversity through the specific litter inputs (Wardle *et al.*, 2004; Trinder *et al.*, 2009; Millard & Singh, 2010), or microclimate modifications in temperature and moisture, which may also vary among plant species (Angers & Caron, 1998; Maestre *et al.*, 2009). Furthermore, it is also known that abiotic soil factors such as physical structure (Lauber *et al.*, 2009; Rousk *et al.*, 2010; Serna-Chavez *et al.*, 2013), or nutrient stocks (Serna-Chavez *et al.*, 2013; Leff *et al.*, 2015) may also strongly affect microbial diversity. Since the drivers of soil microbial diversity can concurrently be important drivers of plant community structure, soil microbial-plant links can arise (or conversely, be offset) due to the same (or opposite) responses to environmental conditions. An important challenge is, therefore, to unravel whether the influence of the root community on microbial diversity parallels or, alternatively, goes beyond the effect of the aerial canopy and the soil physicochemical properties.

In this study, we evaluated the role of plant roots as drivers of soil microbial diversity. We specifically assessed the effects of richness of the root communities, their species composition and biomass, on both the richness and species composition of soil fungal and bacterial communities. We also assessed the coupling of root and microbial β-diversity. Because the associations between root and microbial communities can also be due to shared responses to other concomitant factors, we examined root-microbial relationships after accounting for the effects of plant aboveground and soil physicochemical properties. In addition, because both microbial communities and environmental factors, including non-measured ones, such as topography or soil moisture content, frequently have a predictable spatial structure (Ettema & Wardle, 2002), we also considered the role of explicit spatial covariates. For this purpose, we combined DNA metabarcoding techniques with spatially explicit sampling in a Mediterranean

scrubland, considering the scale at which plant to plant interactions occur in this community (Chacón-Labella *et al.*, 2016; Pescador *et al.*, 2020). Specifically, we address the following questions: (1) Which root community attributes (root richness, biomass, composition and β-diversity) predict the patterns of microbial diversity? (2) Do root community attributes explain more variation in the microbial community structure than the aboveground component, soil physicochemical properties, and other spatially structured factors?

Methods

Study area, vegetation and soil sampling

The study was conducted in a species-rich semiarid Mediterranean scrubland near Orusco de Tajuña (Madrid, Spain) in the central Iberian Peninsula. The climate is semiarid Mediterranean with a mean annual precipitation of 452 mm, summer drought and a mean temperature of 12.8°C. The soil is characterized as Xeric Calcigypsids (Soil Survey Staff, 2014) with low gypsum content (<10%). The plant community is very rich -48 perennial species found in a 60 m^2 plot in Chacón-Labella *et al.* (2016), including a diverse assemblage of chamaephytes such as *Thymus vulgaris* L., *Bupleurum fruticescens* Loefl. ex L., *Helianthemum cinereum* (Cav.) Pers., *Fumana ericoides* (Cav.) Gand. and *Linum suffruticosum* L. and perennial grasses such as *Stipa pennata* L., *Avenula bromoides* (Gouan) H. Scholz and *Koeleria vallesiana* (Honck.) Gaudin. Sparse sprouting shrubs such as *Quercus coccifera* L. and, occasionally, *Quercus ilex* subsp. *ballota* (Desf.) Samp. trees are common in the area.

In May 2016, we established an 8 × 8 m plot (40°16'08.5"N 3°08'11.1"W; 781 m a.s.l.) representative of the dominant vegetation on a northwest-facing slope (<11°) in a homogeneous area. The mean perennial plant cover in this area was around 40%. The plot size guaranteed the inclusion of a high number of species (45) and individuals (8551). Within this plot, each perennial plant, except for seedlings, was mapped with 1 cm absolute precision using a Leica Real-Time-GPS (Viva GS15, Leica, Wetzlar, Germany). The projection area of the crown of each individual plant was approximated by a circle with radius r = (L+S)/4, where L is the longest diameter of the crown and S its perpendicular diameter. Within this plot, we also set 64 sampling points on an 8 × 8 regular grid (i.e. 1 m spacing/distance between contiguous sampling points). We set 20 additional sampling points in four groups at the corners of the plot to increase the spatial resolution, resulting in 0.70 m spacing between sampling points in these areas (see Fig. S1 for more details). We georeferenced the centre of each sampling point using the Leica Real-Time-GPS.

Around each sampling point, two contiguous soil samples were collected using steel cores of 5 cm diameter x 10 cm depth. The sampling depth of the cores was chosen based on the distribution of root biomass in the soil in this plant community, which is significantly higher in the first 10 cm than in the deeper 10-30 cm layer (data not shown), therefore allowing sampling of a large proportion of the belowground plant community in the plot. One sample was employed to assess the soil microbial community and soil physicochemical variables (hereafter soil-microbial samples) and the second one to study the belowground plant community (hereafter root samples). Soils from the soil-microbial samples were thoroughly sieved through a 2-mm mesh, homogenized and separated into two subsamples: 1 g of homogenized soil for molecular analyses, and 50 g of air-dried soil for soil physicochemical analyses. Plant roots from each root sample were thoroughly washed, in the first 48 hours since field collection. The root material was centrifuged at 3000 rpm for 30 seconds to remove excess water, weighed to estimate fresh root biomass per core (hereafter root biomass) and homogenized by cutting roots in small pieces. A portion of 0.1 g of fresh root biomass per sample was stored at -80 ºC for subsequent DNA metabarcoding analyses.

Soil microbial community

The identification and estimation of the abundances of the fungal and bacterial OTUs was assessed in each soil-microbial sample through DNA metabarcoding, as explained in Methods S1. In brief, DNA was isolated in the 84 soil-microbial samples using the DNeasy PowerSoil isolation kit (Qiagen, CA, USA) from 0.25 g of dry soil. The bacterial 16S rRNA gene and the fungal ITS2 region were sequenced in the Illumina MiSeq PE300 v3 run at the Unidad de Genómica (Fundación Parque Científico de Madrid, Spain). After assessment of the quality of the Illumina raw reads using FastQC (Andrews 2010), and the paired-end assembly of the R1 and R2 reads with FLASH (Magoč & Salzberg 2011), sequences were quality-filtered (minimum Phred quality score of 20) and labelled using the *multiple_split_libraries.py* script implemented in Qiime (Caporaso *et al.* 2010). Bioinformatic analyses were conducted using the VSEARCH tool (Rognes *et al.* 2016). Sequences were dereplicated (-derep fulllength), clustered at a similarity threshold of 100% (-cluster fast, {centroids option), and sorted (-sortbysize). A quality-filtering was applied to the OTU tables to remove the OTUs occurring at a frequency below 0.005% in the whole dataset and the low abundance OTUs of each soil-microbial sample (0.1% threshold).

Before conducting further analyses, bacterial and fungal reads were rarefied to the minimum number of sequences in a soil-microbial sample for each microbial group (i.e. 2350 and 11872 sequences per sample respectively, Fig. S2), to account for the unequal number of sequences between samples. Since methodological biases (extraction bias, amplification bias,

sequencing bias) may hinder an accurate estimation of actual abundances, the microbial community matrix was Hellinger-transformed (Legendre & Gallagher, 2001). This transformation, which involves that the abundance values of each OTUs are first divided by the sample total abundance, and the result is square-root transformed, downweights the importance of species abundance (Legendre & Gallagher, 2001) and avoids the double-zero asymmetry (Legendre & Legendre, 2012).

Belowground and aboveground plant community

Belowground plant community was assessed following the DNA metabarcoding protocol described in Matesanz *et al.* (2019). In brief, DNA was extracted from 0.1 g of the homogenized root tissue of each root sample using the DNEasy Plant Minikit (Qiagen, CA, USA). A fragment of the *rbcL* chloroplast gene (550 bp) was sequenced in the Illumina MiSeq PE300 run. After assessment of the quality of the Illumina raw reads using FastQC, the R1 and R2 reads were quality-filtered using Geneious 11.1.2 (www.geneious.com), trimmed according to the average Phred score (minimum Phred quality score of 20), and concatenated using the fuse.sh script implemented in the 'BBmap' package (Bushnell, 2014). The sequences were labelled (demultiplexed) using the script multiple split libraries.py implemented in Qiime (Caporaso *et al.*, 2010). Sequences were dereplicated (-derepfullength), clustered at a similarity threshold of 100% (-cluster fast,-centroids option), and sorted (-sortbysize). Chimera sequences identified by the UCHIME algorithm implemented in VSEARCH were discarded (Edgar *et al.*, 2011). Taxonomic assignment of sequences was done using the -usearch global option of VSEARCH and considering a 99% similarity threshold, from an in-house reference database with the *rbcL* sequences of 45 plant species from 18 families found in the study area. *rbcL* was able to identify individual species in most cases, except for a few very close relatives such as *Thymus vulgaris* L., *T. lacaitae* Pau, *Stipa pennata, S. tenacissima* L.*, Teucrium capitatum* L.*, T. gnaphalodes* L'Hér. Stirp*, Quercus coccifera* and *Q. ilex*, which were grouped at the genus level. One root sample that rendered only one sequence read was excluded from further analyses. The number of sequences assigned to each plant species was used as an estimate of its abundance in each sample.

Aboveground plant abundance (i.e., plant cover) was estimated as the sum of all the intersection areas between the projection of the crown of each individual plant and a circle of 20 cm radius around each sampling point (Fig. S3). This radius was selected as the one that maximized the similarity between aboveground and belowground samples (A. Illuminati *et al.*, unpublished).

Soil physicochemical variables

Soil physicochemical analyses were conducted as described by López-Angulo *et al.* (2018). Briefly, we analysed four nutrient stocks: soil organic carbon (SOC), total nitrogen (N), available phosphorus (P) and potassium (K); two dynamic variables related to the soil microbial activity such as acid phosphatase and β-glucosidase enzymatic activities; and several variables such as pH, electrical conductivity, sand, silt and clay contents (Table S1). SOC was determined by colorimetry, and Total N and available P using a SKALAR San++ Analyser (Skalar, Breda, The Netherlands) after digestion of the soil samples with H_2SO_4. K, pH, and electrical conductivity were measured in water suspension. Phosphatase and β-glucosidase activities were estimated as described in Tabatabai (1982). Sand (2.0-0.05 mm), silt (0.05-0.002 mm) and clay (<0.002 mm) proportions for each soil sample were determined using the methods described by Kettler *et al.* (2001). Prior to statistical analyses, soil organic C, phosphatase activity, conductivity and clay content were log-transformed, and β-glucosidase activity was square root-transformed to approximate normal distributions. All soil physicochemical variables were standardized and submitted to a Principal Component Analysis (PCA) with varimax rotation to reduce the number and multicollinearity of the soil predictor variables and maximize their correlation with the PCA components. Four PCA components (accounting for 75% of variance; see Table S2), all of them with sound ecological meaning, were considered in further analyses as predictors representing different important soil features. They, respectively, represented variation in texture (negatively correlated with sand, and positively with silt and clay; 22% of variance), soil organic carbon (19%), fertility (positively correlated with nitrogen and phosphorus; 18%) and salinity (negatively correlated with pH and positively with conductivity; 16%).

Spatial variables

To account for any additional variation in the microbial communities not explained by below- and aboveground plant communities and soil physicochemical properties, we generated a set of Moran´s eigenvectors from the coordinates of each sampling point using distance-based Moran's eigenvectors maps (dbMEM; Legendre & Legendre, 2012). This technique uses Principal Coordinates Analysis to generate orthogonal eigenvectors of truncated matrices of geographical distances among sites, allowing us to assess simultaneously multiple spatial structures (Borcard & Legendre, 2002). The first dbMEM eigenvectors reflect broader spatial structures, while later dbMEM vectors represent finer spatial structures (Borcard & Legendre, 2002). We selected a parsimonious set of dbMEM eigenvectors related to richness and species composition (detrended Hellinger-transformed data) of each microbial community (bacteria and fungi), applying a forward selection with double-stopping criterion (α = 0.05, 9999

permutations) (Blanchet *et al.*, 2008). Significant linear trends were removed by univariate (microbial richness) and multivariate (microbial composition) regressions, and the detrended residuals were then used as response variables (Borcard & Legendre, 2002). Both the linear trend (XY coordinates) and dbMEM eigenvectors were considered as spatial variables in the statistical analyses.

Statistical analyses

Plant community predictors

Several attributes of the plant community were considered as predictors of microbial diversity: below- and aboveground richness, composition, β-diversity and abundance. Below- and aboveground plant richness were estimated as the number of plant species in each root sample and sampling circle, respectively. Below- and aboveground plant composition (two descriptors for each plant component above- and belowground, hereafter composition.1 and composition.2; Fig. S4) were estimated as the scores of each sample on the axes of a non-metric multidimensional scaling ordination (nMDS). To compute these ordinations, we employed the matrices of pairwise Bray-Curtis dissimilarity based on the sequence reads of each species in the root sample and the cover of each species occurring in the sampling circle, respectively. When the response of microbial richness to plant composition was evaluated, we used presence/absence plant data instead of the abundance data to quantify plant composition. This ensured consistency with the diversity index assessed (i.e. richness, not abundance-weighted alpha diversity).

Plant β-diversity (compositional dissimilarity between root samples) was estimated as the matrix of pairwise Bray-Curtis composition dissimilarity between samples (Jost *et al.*, 2011). Furthermore, below- and aboveground abundance were considered as the total root biomass per root sample, and the total plant cover per circle, respectively. Both plant cover and the number of sequences reads were log10-transformed before analysis. Finally, we examined the correlation between below- and aboveground plant community attributes prior to statistical analyses (Fig. S5) corroborating the decoupling between both plant compartments (A. Illuminati *et al.*, unpublished).

Bacterial and fungal richness

To evaluate the variation in bacterial and fungal richness (i.e. the total number of OTUs) explained by the below- and aboveground plant community attributes, and their shared variation with the soil properties and spatial covariates, we used a variance partitioning analysis (Borcard *et al.*, 1992). We introduced in this analysis only the most “important variables” of

each of our four sets of predictors (below- and aboveground plant component, soil properties and space). Important variables were selected using a model selection procedure based on the sum of Akaike weights. We first fitted Poisson generalized linear models (GLMs), one for each of the four sets of predictors (Table S3). Then, for each GLM (and each set of predictors), we selected the subset of models with strongest empirical support on the basis of the corrected Akaike information criterion (AIC_c), i.e. we selected the model with the smallest AICc and any other model which differed from it less than 2 AICc units (Burnham & Anderson, 2002). For all the selected models, we calculated Akaike weights (w_+), i.e. the probability that the model is the best model from the subset considered (Burnham & Anderson, 2002). Then, for each predictor, we estimated its relative importance (w_i), by summing w_+ values of all the selected models in which the predictor appeared (Burnham & Anderson, 2002). Finally, following Burnham (2015), from each of the four sets of predictors, we included in the final variance partitioning only those predictors with $w_i > 0.4$ (i.e., the "important variables").

Furthermore, we evaluated the effect of belowground and aboveground plant community attributes (richness, species composition and root biomass) on soil bacterial and fungal richness. For this, all variables from each set were included in a final Poisson GLM for bacterial and fungal richness (Table S4). We calculated model-averaged parameter estimates over the set of models with ΔAICc<2, weighting single-model estimates by their Akaike weights (Burnham & Anderson, 2002). We estimated 95% confidence intervals (CI) around model-averaged parameter estimates, and we considered a parameter to be significant if the 95% CI excluded zero (Burnham & Anderson, 2002). We checked model assumptions by examining the correlation matrix between predictors (Table S5) and assessed the absence of multi-collinearity in all models (Table 1 and S3) using the variance inflation factor (VIF). In all cases, VIFs values were smaller than 4, suggesting the absence of collinearity problems (Zuur *et al.*, 2010). To avoid overparameterization, a maximum of eight predictors were allowed in the candidate models (argument 'm.lim'; function 'dredge; package 'MuMIn').

Bacterial and fungal community composition

We assessed the variation in bacterial and fungal composition (soil-microbial sample × species abundance data) explained by the below- and aboveground plant community attributes, and their shared variation with the soil properties and space covariates using, again, the variance partitioning analysis. We first conducted a forward selection with double-stopping criteria ($p< 0.05$ and adjusted R^2 < global R^2; Blanchet *et al.*, 2008) based on a partial RDA analysis (pRDA; Legendre *et al.* 2012), to select which variables from each of the four sets of predictors to be included in the variance partitioning. Finally, we tested the significance of

predictors in the pRDAs using the Monte Carlo test based on 999 permutations. RDA was chosen instead of CCA because it was less sensitive to species with clumped distributions and low abundance.

Bacterial and fungal β-diversity

To test the effect of belowground plant community β-diversity (i.e. compositional dissimilarity between soil-microbial samples) on microbial β-diversity, we used two complementary statistical approaches. We first applied a variance partitioning analysis to quantify the pure contribution of belowground plant β-diversity to variation in microbial β-diversity using distance-based redundancy analysis (dbRDA: Borcar*d et al* 1992). The total variation of fungal and bacterial β-diversity was partitioned based on R^2 statistics derived from dbRDAs. We then assessed whether dissimilarity in belowground plant composition correlated with dissimilarity in microbial composition using partial Mantel tests to control for the potential confounding effects due to dissimilarity in aboveground plant composition and soil properties and to spatial distance among samples. Dissimilarities in plant (above- and belowground) and microbial (bacterial and fungal) composition between samples were estimated as Bray-Curtis distance after Hellinger-transformation. Dissimilarity in soil properties and spatial distance between samples were estimated as Euclidean distance using 11 soil variables and X-Y coordinates, respectively. All analyses were performed in R (R Core Team) and a detailed description of packages used can be found in Methods S2.

Results

Taxonomic description of the microbial and plant communities

We found 1339 bacterial and 835 fungal OTUs across all samples. Bacterial and fungal richness per sample ranged from 181 to 246 OTUs (212 ± 13 on average; mean ± SD) and 31 to 133 OTUs (83 ± 17) respectively. The bacterial community was dominated by Actinobacteria, with Proteobacteria being the second most abundant bacterial phylum (60% and 23% respectively, Fig. S6). The dominant bacterial classes were Thermoleophilia, Alphaproteobacteria, Rubrobacteria and Actinobacteria, representing 5.29%, 2.88%, 1.45% and 1.13% of the sequences, respectively (Table S6). Ascomycota was the dominant fungal phylum followed by Basidiomycota (76% and 22% of the fungal ITS2 sequences respectively, Fig. S4). The most abundant fungal classes across samples were Pezizomycetes, Eurotiomycetes, Agaricomycetes and Dothideomycetes, representing 19.2%, 16.9% 14.8% and 8.6% of the total number of sequences, respectively (Table S7).

In the case of the plant community, a total of 30 plant taxa, 26 identified at the species level and 4 at the genus level, were found across all soil samples (estimated from DNA metabarcoding), while 38 plant species were detected aboveground, in the area that corresponded to circles with 20 cm radius. Aboveground plant cover in the circles ranged from 0.35 to 17.5% per circle (4.5 ± 3.3%) while root biomass in the root samples ranged from 0.75 to 6.80 g (7 ± 2 g). The taxa more frequently encountered belowground were *Thymus* sp. (present in 86% of the root samples), *Quercus* sp. (81%), *Stipa* sp. (71%) and *Linum suffruticosum* (51%). Aboveground, the most frequent species in the circles were *Stipa* sp. (93%), *Thymus* sp. (82%), *Helianthemum cinereum* (Cav.) Pers (78%) and *Linum suffruticosum* L. (71%).

Bacterial and fungal richness

The models explained 16.1% and 13.9% of the total variance of bacterial and fungal richness, respectively (Fig. 1). Belowground (i.e. roots) plant community composition explained 4.9% of bacterial richness variance (Fig. 1), but belowground community composition and root biomass together explained only 1.4% of the variance in fungal richness (Fig. 1). Fungal richness was positively related to root biomass (Fig. 2). Soil fertility (Table S2) affected the richness of both microbial groups, but the direction of its effects was positive for bacterial, and negative for fungal richness (Table 1). The spatial structure represented by the dbMEM 29 (fine spatial scale) exerted significant effects on fungal richness, while dbMEM 9 (broad spatial scale) did so on bacterial richness (Table 1).

Bacterial and fungal community composition

Variance partitioning analyses showed that the predictors explained 7.8% and 18.8 % of the total variance of bacterial and fungal composition (Fig. 1), respectively. The unique fractions of variation in bacterial and fungal composition explained by the forward-selected belowground plant community attributes (root biomass and root composition.1; Table 2) were respectively 0.5% and 0.3% (Fig. 1). After accounting for the effects of the aboveground composition, soil variables and spatial covariates (Table 2), the partial RDA revealed that the bacterial composition was significantly affected by root composition.1 (Table 2). Partial RDAs showed that fungal but not bacterial composition was associated with variations in aboveground plant composition and soil properties (soil organic carbon and soil texture: 1^{st} and 2^{nd} PCA axes, Table S2). We also found that the spatial trend (X-Y coordinates), and other spatial variables related to fine and broad scales (e.g. dbMEM 2 and 29) were significantly associated with differences in bacterial and fungal composition (Table 2).

Bacterial and fungal β-diversity

Variance partitioning showed that the β-diversity of the below- and aboveground plant communities, the soil properties and the spatial covariates explained 13.6% and 23.8% of the total variance of bacterial and fungal β-diversity, respectively. Specifically, β-diversity based on root distributions explained 2.1% and 0.5% of the variation in bacterial and fungal β-diversity respectively (Fig. 1). Partial Mantel tests also showed that belowground plant β-diversity was significantly correlated with bacterial β-diversity (Spearman *rho* = 0.13, p = 0.024, Fig. 3, Table S8) but not correlated with fungal β-diversity (Spearman *rho* = 0.09, p = 0.114, Fig. 3). In other words, the more different the root composition, the more different the bacterial composition among samples. In contrast, partial Mantel test revealed that the more similar the fungal communities were between two sites (i.e. the lower their fungal β-diversity), the more similar their aboveground plant β-diversity was (Spearman *rho*= 0.12, p = 0.009, Fig. 3). We also found that bacterial β-diversity was significantly correlated with the dissimilarity in soil properties between samples (Spearman *rho* = 0.18, p = 0.004). After controlling for soil properties and β-diversity of both plant components, spatial distance between samples was significantly correlated with microbial β-diversity (bacteria: Spearman *rho* = 0. 22, $p < 0.001$; fungi: *rho* = 0.37, $p < 0.001$).

Discussion

Our results from a semiarid Mediterranean scrubland provide empirical evidence that the diversity of microbial soil communities changes in response to variations in the belowground plant community. We found that fungal richness increased with greater root biomass (Fig. 4a), while bacterial richness and composition were affected by the variations in root composition (Fig. 4b). Importantly, the effects of roots composition and biomass were not redundant with the effect of the aboveground plant community, the soil physicochemical properties and the spatial covariates. However, we only found an association between the β-diversity of roots and bacteria, but not fungi (Fig. 4c). Altogether, our study shows that roots exerted different effects on each microbial group, which are independent from the aboveground inputs, soil properties or other non-measured factors (estimated as spatial covariates). This novel finding highlights that information of both below- and aboveground community attributes should be incorporated for a more complete understanding of complex soil microbiome-plant interactions at the scale in which semiarid scrubs interact..

Root community attributes explain patterns in soil microbial communities

Root composition, i.e. the identity of plant roots, was the only plant predictor able to explain bacterial species richness estimated as the number of bacterial OTUs in the soil. This

relationship may be explained by changes in the type of the root exudate compounds delivered to the soil by different plant species (Haichar *et al.*, 2008; Shi *et al.*, 2011). We also found that the composition of roots contributed to structure the bacterial community composition, which has also been reported in other studies (Haichar *et al.*, 2008; Van Der Heijden *et al.*, 2008; Berg & Smalla, 2009). In addition, bacterial β-diversity was positively associated with β-diversity of root assemblages, suggesting that certain taxa of soil bacteria and plants tended to co-occur in the soil. A plausible explanation of these results might be based on the differences in their competitive abilities. Certain root exudates, more efficiently exploited by particular bacteria taxa, could lead to a reduction in the number of other bacterial species via competitive exclusion. Accordingly, other rhizodeposits derived from different plant species could sustain species-rich bacterial communities, reducing the competitive exclusion and promoting bacterial coexistence (Goberna *et al.*, 2016). In addition to chemical and physiological root traits related to rhizodeposits, both structural and anatomical root traits may contribute to patterns of bacterial richness and composition (Legay *et al.*, 2014; Gould *et al.*, 2016), especially considering their influence on the recognition and adherence of plant-associated bacteria to plant roots (Berg & Smalla, 2009). Alternatively, other environmental changes caused by roots such as variations in ion concentration or the synthesis and liberation of some antimicrobial metabolites might also influence the structure of the bacterial communities (Dakora & Phillips, 1996; Berg & Smalla, 2009; Philippot *et al.*, 2013; Gould *et al.*, 2016).

Our findings also highlight the potential role played by roots as driver of fungal richness. Specifically, root biomass was the only belowground attribute able to explain a significant fraction of variation in fungal richness. This suggests that fungal richness is more related to the amount of resources than to its variety (i.e. richness) or type (i.e. composition) (Eisenhauer *et al.*, 2017). Furthermore, the composition of the bacterial and fungal communities responded differently to belowground plant composition, as has been reported elsewhere (Burns *et al.*, 2015; Leff *et al.*, 2018). This result highlights the importance of intimate interactions between specific plants and associated fungi and bacteria, and reinforces the role of rhizodeposition as a mechanism of ongoing coevolutionary processes between plants and microbes (De-la-Peña *et al.*, 2008; Badri & Vivanco, 2009). In this context, quantifying the functional role of different roots (and their rhizodeposits) while accounting for their phylogenetic relatedness, could provide further insights into plant-microbial relationships (Tedersoo *et al.* 2013; Legay *et al.* 2014; but see: Barberán *et al.* 2015; Leff *et al.* 2018).

Surprisingly, bacterial and fungal richness did not vary according to belowground (or aboveground) plant richness. Theoretically, it could be expected that a more species-rich plant

assemblage, which provides a higher diversity of resources would favour niche partitioning, lead to a richer soil microbial community (De Boer *et al.*, 2005; Wardle, 2006; Eisenhauer *et al.*, 2010). However, this lack of relationship between plant and soil microbial richness has been previously reported in both experimental and observational studies of bacteria and fungi conducted at very different ecosystems and spatial scales (Waldrop *et al.*, 2006; Wardle, 2006; Tedersoo *et al.*, 2014; Prober *et al.*, 2015; Delgado-Baquerizo *et al.*, 2018). This decoupling has been attributed to different causes, from low variation in plant richness in local-scale studies (see Delgado-Baquerizo *et al.* 2018), to the blurring of the local effects of plant richness in global-scale studies (Prober *et al.*, 2015). In our study, the decoupling between microbial and plant diversity may also be due to the existence of strong abiotic filters in our plant community (semiarid climate and gypsum soil) that may reduce trait variability among plant species (Escudero *et al.*, 2015; Pescador *et al.*, 2018; Peralta *et al.*, 2019), decreasing the range of variability of resources (Wardle *et al.*, 2004; Orwin *et al.*, 2010).

Relative importance of roots versus aboveground plant community, soil heterogeneity and space

Although our results show that root community attributes play a role in soil microbial diversity, other predictors such as soil, space, and the aboveground plant community attributes consistently explained larger fractions of variation in microbial richness, composition or β-diversity (Fig. 1). For example, we found a clear response of fungal communities to the variation in the aboveground plant community. More specifically, fungal richness and composition responded to the aboveground plant composition. This suggests that the number of fungal species and their identity is more sensitive to changes in the chemistry of the aboveground litter resulting from differences in plant community composition (Trinder *et al.*, 2009) than to variation in the chemical rhizodeposition. In addition, aboveground plant β-diversity predicted the fungal β-diversity even after accounting for the root β-diversity, soil properties and the spatial variation. The differential responses found for fungal and bacterial communities suggest that plant communities exert different influences on both microbial groups, mediated by the above- and belowground counterparts. Having faster growth strategies, bacteria probably exploit low-molecular-weight organic compounds derived from exudates, whereas fungi could be more strongly related to the degradation of highly polymeric compounds like lignin or cellulose (Tuomela *et al.*, 2000; Lynd *et al.*, 2002; De Boer *et al.*, 2005; Legay *et al.*, 2014).

Soil physicochemical properties had the most prominent role on bacterial diversity (Fig. 1), playing a weaker role on fungal diversity. Soil fertility positively affected bacterial richness, but negatively affected fungal richness. These results, which support the existence of resource partitioning, are in line with studies that reported a decrease in the fungal:bacterial biomass

ratio in soils with high nitrogen and phosphorus content (de Vries *et al.*, 2006, 2012). On the other hand, spatial covariates explained the largest fraction of the variation in fungal richness, composition and β-diversity, i.e. a significant fraction of this variance was related to environmental factors not directly measured in the field or to endogenous processes such as dispersal. Thus, our results show that the microbial communities in this semiarid Mediterranean scrubland are spatially structured, in agreement with previous studies conducted in other systems (Klironomos *et al.*, 1999; Stegen *et al.*, 2015). Furthermore, the effect of dbMEM spatial eigenfunctions provides evidence that the spatial patterns in bacterial richness vary at broader spatial scales than fungal richness (scale size *sensu* Legendre *et al.* 2012). This again highlights the occurrence of different additional factors shaping the richness and composition patterns of both microbial guilds. For instance, the broader spatial patterns of bacterial richness could be shaped by the variation of key soil micronutrients (e.g. concentration of aluminum or calcium: Barberán *et al.* 2015), while the fungal spatial patterns may be caused by processes occurring at finer spatial scales, including interactions across trophic groups (e.g. fungal-feeding nematodes: Wardle & Yeates 1993; Wardle 2006). Finally, although dispersal limitation could be expected to be negligible given the spatial extent of the sampling area (Abu-Ashour *et al.*, 1994), partial Mantel tests showed that fungal β-diversity was more strongly related to spatial distance than bacterial β-diversity (Table S8), which suggests that bacteria have higher dispersal abilities than fungi (Abu-Ashour *et al.*, 1994; Yang & van Elsas, 2018). This result agrees with previous evidence that bacteria may be transported by water flow (Abu-Ashour *et al.*, 1994; Yang & van Elsas, 2018), while fungi depend mainly on hyphal extension (Wardle 2006). Finally, it is also noteworthy that models did not explain large fractions of variance of the microbial richness, composition and β-diversity (from 76.2 % to 92.2 % unexplained variance, Fig. 1). This could be related to the effect of other micro-scale factors, including the distribution of micro-aggregates and micro-pores in the soil (Vos *et al.*, 2013), and/or the demographic stochasticity of microbial communities (Stegen *et al.*, 2012; Zhou, 2017).

Conclusion

Our study highlights the key and independent role of plant roots for explaining the variation in soil microbial diversity in a semiarid Mediterranean scrubland. For the first time, we show that unique fractions of variation in microbial richness, composition and β-diversity can only be explained by the type (root composition) and amount (root biomass) but not the variety (root richness) of root assemblages. Furthermore, our results provide new insights into the effects of the aboveground plant community on the structure of the soil fungal and bacterial communities. In particular, aboveground plant composition, but not root composition, affected

fungal composition and richness. Our findings also advance our understanding of how the soil physicochemical properties, through variations in fertility, carbon and texture, can predict changes in the composition and richness of the soil microbial communities. Our study highlights the role of plant distribution both below- and aboveground in explaining heterogeneity in soil microbial diversity and suggests that incorporating data on both plant compartments will further our understanding of the relationships between soil microbial and plant communities. This is particularly crucial in water-limited ecosystems, where a decoupling between the aboveground and belowground distribution of plant community attributes often occurs (Schenk & Jackson, 2002; Mokany *et al.*, 2006).

Acknowledgements

We thank Carlos Díaz for technical assistance in the field, AllGenetics & Biology (https://www.allgenetics.eu/) for molecular analyses, and Pilar Hurtado for assistance with Fig. 4. We also thank four anonymous reviewers for useful comments and suggestions. This study was supported by the Ministerio de Economía y Competitividad de España (grant PHENOTYPES, PGC2018-09915-B-100; and ROOTS, CGL2015-66809-P) and Comunidad de Madrid (grant REMEDINAL TE-CM, S2018/EMT-4338). JLA was supported by a post-doctoral contract (M1718-178) from the Consejería de Educación, Juventud y Deporte de la Comunidad de Madrid and the European Social Fund.

Author contributions

AE planned and designed the research. JC-L, SM, AI, DSP, BP, AS, MC and JL-A conducted field and lab work. JL-A conducted data statistical analyses and wrote the manuscript with extensive input from the rest of authors.

Data availability statement

Data associated with this paper has been deposited in figshare: http://figshare.com/s/ (10.6084/m9. figshare.) Illumina next-generation DNA sequences have been deposited in the Sequencing Read Archive (SRA) of the National Centre for Biotechnology Information under Bioproject accession sada

References

Abu-Ashour J, Joy DM, Lee H, Whiteley HR, Zelin S. 1994. Transport of microorganisms through soil. *Water, Air, & Soil Pollution* 75: 141–158.

Adamczyk M, Hagedorn F, Wipf S, Donhauser J, Vittoz P, Rixen C, Frossard A, Theurillat JP, Frey B. 2019. The soil microbiome of Gloria Mountain summits in the Swiss Alps. *Frontiers in*

582 *Microbiology* **10**.

583 **Angers DA, Caron J. 1998**. Plant-induced changes in soil structure: processes and feedbacks.
584 *Biogeochemistry* **42**: 55–72.

585 **Badri D V., Vivanco JM. 2009**. Regulation and function of root exudates. *Plant, Cell and*
586 *Environment* **32**: 666–681.

587 **Barberán A, Mcguire KL, Wolf JA, Jones FA, Wright SJ, Turner BL, Essene A, Hubbell SP, Faircloth**
588 **BC, Fierer N. 2015**. Relating belowground microbial composition to the taxonomic, phylogenetic,
589 and functional trait distributions of trees in a tropical forest. *Ecology Letters* **18**: 1397–1405.

590 **Bardgett RD, Bowman WD, Kaufmann R, Schmidt SK. 2005**. A temporal approach to linking
591 aboveground and belowground ecology. *Trends in Ecology and Evolution* **20**: 634–641.

592 **Bardgett RD, Van Der Putten WH. 2014**. Belowground biodiversity and ecosystem functioning.
593 *Nature* **515**: 505–511.

594 **Berg G, Smalla K. 2009**. Plant species and soil type cooperatively shape the structure and
595 function of microbial communities in the rhizosphere. *FEMS Microbiology Ecology* **68**: 1–13.

596 **Blanchet FG, Legendre P, Borcard D. 2008**. Forward selection of explanatory variables. *Ecology*
597 **89**: 2623–2632.

598 **De Boer W, Folman LB, Summerbell RC, Boddy L. 2005**. Living in a fungal world: Impact of fungi
599 on soil bacterial niche development. *FEMS Microbiology Reviews* **29**: 795–811.

600 **Borcard D, Legendre P. 2002**. All-scale spatial analysis of ecological data by means of principal
601 coordinates of neighbour matrices. *Ecological Modelling* **153**: 51–68.

602 **Borcard D, Legendre P, Drapeau P. 1992**. Partialling out the spatial component of ecological
603 variation. *Ecology* **73**: 1045–1055.

604 **Broeckling CD, Broz AK, Bergelson J, Manter DK, Vivanco JM. 2008**. Root exudates regulate soil
605 fungal community composition and diversity. *Applied and Environmental Microbiology* **74**: 738–
606 744.

607 **Burnham KP. 2015**. *Multimodel Inference: understanding AIC relative variable importance values*.
608 [WWW document] URL https://https://sites.warnercnr.colostate.edu/kenburnham/wp-
609 content/uploads/sites/25/2016/08/VARIMP.pdf [accessed 1 June 2020].

610 **Burnham KP, Anderson DR. 2002**. *Model selection and multimodel inference: a practical*
611 *information-theoretic approach*. New York, USA: Springer.

612 Burns JH, Anacker BL, Strauss SY, Burke DJ. 2015. Soil microbial community variation correlates
613 most strongly with plant species identity, followed by soil chemistry, spatial location and plant
614 genus. *AoB PLANTS* **7**: 1–10.

615 Bushnell B. 2014. *BBMap: a fast, accurate, splice-aware aligner*. Berkeley, CA, USA: Lawrence
616 Berkeley National Lab. (LBNL).

617 Caporaso JG, Kuczynski J, Stombaugh J, Bittinger K, Bushman FD, Costello EK, Fierer N, Pena AG,
618 Goodrich JK, Gordon JI. 2010. QIIME allows analysis of high-throughput community sequencing
619 data. *Nature methods* **7**: 335.

620 Chacón-Labella J, de la Cruz M, Escudero A. 2016. Beyond the classical nurse species effect:
621 Diversity assembly in a Mediterranean semi-arid dwarf shrubland. *Journal of Vegetation Science*
622 **27**: 80–88.

623 Chen L, Xiang W, Wu H, Ouyang S, Zhou B, Zeng Y, Chen Y, Kuzyakov Y. 2019. Tree species identity
624 surpasses richness in affecting soil microbial richness and community composition in subtropical
625 forests. *Soil Biology and Biochemistry* **130**: 113–121.

626 Dakora FD, Phillips DA. 1996. Diverse functions of isoflavonoids in legumes transcend anti-
627 microbial definitions of phytoalexins. *Physiological and Molecular Plant Pathology* **49**: 1–20.

628 De-la-Peña C, Lei Z, Watson BS, Sumner LW, Vivanco JM. 2008. Root-microbe communication
629 through protein secretion. *Journal of Biological Chemistry* **283**: 25247–25255.

630 Delgado-Baquerizo M, Fry EL, Eldridge DJ, de Vries FT, Manning P, Hamonts K, Kattge J, Boenisch
631 G, Singh BK, Bardgett RD. 2018. Plant attributes explain the distribution of soil microbial
632 communities in two contrasting regions of the globe. *New Phytologist* **219**: 574–587.

633 Delgado-Baquerizo M, García-Palacios P, Milla R, Gallardo A, Maestre FT. 2015. Soil
634 characteristics determine soil carbon and nitrogen availability during leaf litter decomposition
635 regardless of litter quality. *Soil Biology and Biochemistry* **81**: 134–142.

636 Edgar RC, Haas BJ, Clemente JC, Quince C, Knight R. 2011. UCHIME improves sensitivity and
637 speed of chimera detection. *Bioinformatics* **27**: 2194–2200.

638 Eisenhauer N, Beßler H, Engels C, Gleixner G, Habekost M, Milcu A, Partsch S, Sabais ACW,
639 Scherber C, Steinbeiss S. 2010. Plant diversity effects on soil microorganisms support the
640 singular hypothesis. *Ecology* **91**: 485–496.

641 Eisenhauer N, Lanoue A, Strecker T, Scheu S, Steinauer K, Thakur MP, Mommer L. 2017. Root
642 biomass and exudates link plant diversity with soil bacterial and fungal biomass. *Scientific*

643 *Reports* 7: 1–8.

644 Escudero A, Palacio S, Maestre FT, Luzuriaga AL. 2015. Plant life on gypsum: a review of its
645 multiple facets. *Biological Reviews* 90: 1–18.

646 Ettema CH, Wardle DA. 2002. Spatial soil ecology. *Trends in Ecology and Evolution* 17: 177–183.

647 Fierer N, Ladau J, Clemente JC, Leff JW, Owens SM, Pollard KS, Knight R, Gilbert JA, McCulley RL.
648 2013. Reconstructing the microbial diversity and function of pre-agricultural tallgrass prairie
649 soils in the United States. *Science* 342: 621–624.

650 Goberna M, Navarro-Cano JA, Verdú M. 2016. Opposing phylogenetic diversity gradients of plant
651 and soil bacterial communities. *Proceedings Biological Sciences* 283: 20153003.

652 Gould IJ, Quinton JN, Weigelt A, De Deyn GB, Bardgett RD. 2016. Plant diversity and root traits
653 benefit physical properties key to soil function in grasslands. *Ecology letters* 19: 1140–1149.

654 Haichar FEZ, Marol C, Berge O, Rangel-Castro JI, Prosser JI, Balesdent J, Heulin T, Achouak W.
655 2008. Plant host habitat and root exudates shape soil bacterial community structure. *ISME*
656 *Journal* 2: 1221–1230.

657 Hedlund K, Regina IS, Van Der Putten WH, Lepš J, Díaz T, Korthals GW, Lavorel S, Brown VK,
658 Gormsen D, Mortimer SR, *et al.* 2003. Plant species diversity, plant biomass and responses of the
659 soil community on abandoned land across Europe: Idiosyncracy or above-belowground time
660 lags. *Oikos* 103: 45–58.

661 Van Der Heijden MGA, Bardgett RD, Van Straalen NM. 2008. The unseen majority: Soil microbes
662 as drivers of plant diversity and productivity in terrestrial ecosystems. *Ecology Letters* 11: 296–
663 310.

664 Hiiesalu I, Öpik M, Metsis M, Lilje L, Davison J, Vasar M, Moora M, Zobel M, Wilson SD, Pärtel M.
665 2012. Plant species richness belowground: Higher richness and new patterns revealed by next-
666 generation sequencing. *Molecular Ecology* 21: 2004–2016.

667 Jones FA, Erickson DL, Bernal MA, Bermingham E, Kress WJ, Herre EA, Muller-Landau HC, Turner
668 BL. 2011. The roots of diversity: Below ground species richness and rooting distributions in a
669 tropical forest revealed by DNA barcodes and inverse modeling. *PLoS One* 6: e24506.

670 Jones DL, Hodge A, Kuzyakov Y. 2004. Plant and mycorrhizal regulation of rhizodeposition. *New*
671 *Phytologist* 163: 459–480.

672 Jones DL, Nguyen C, Finlay RD. 2009. Carbon flow in the rhizosphere: Carbon trading at the soil-
673 root interface. *Plant and Soil* 321: 5–33.

674 Jost L, Chao A, Chazdon RL. 2011. Compositional similarity and beta diversity. In: Magurran AE,
675 McGill BJ, eds. *Biological diversity: frontiers in measurement and assessment*. Oxford, United
676 Kingdom: Oxford University Press, 66–84.

677 Kernaghan G. 2013. Functional diversity and resource partitioning in fungi associated with the
678 fine feeder roots of forest trees. *Symbiosis* 61: 113–123.

679 Kettler TA, Doran JW, Gilbert TL. 2001. Simplified method for soil particle-size determination to
680 accompany soil-quality analyses. *Soil Science Society of America Journal* 65: 849.

681 Klironomos JN, Rillig MC, Allen MF. 1999. Designing belowground field experiments with the help
682 of semi-variance and power analyses. *Applied Soil Ecology* 12: 227–238.

683 Lauber CL, Hamady M, Knight R, Fierer N. 2009. Pyrosequencing-based assessment of soil pH as a
684 predictor of soil bacterial community structure at the continental scale. *Applied and*
685 *Environmental Microbiology* 75: 5111–5120.

686 Leff JW, Bardgett RD, Wilkinson A, Jackson BG, Pritchard WJ, De Long JR, Oakley S, Mason KE,
687 Ostle NJ, Johnson D, *et al.* 2018. Predicting the structure of soil communities from plant
688 community taxonomy, phylogeny, and traits. *ISME Journal* 12: 1794–1805.

689 Leff JW, Jones SE, Prober SM, Barberán A, Borer ET, Firn JL, Harpole WS, Hobbie SE, Hofmockel KS,
690 Knops JMH, *et al.* 2015. Consistent responses of soil microbial communities to elevated nutrient
691 inputs in grasslands across the globe. *Proceedings of the National Academy of Sciences* 112:
692 10967–10972.

693 Legay N, Baxendale C, Grigulis K, Krainer U, Kastl E, Schloter M, Bardgett RD, Arnoldi C, Bahn M,
694 Dumont M, *et al.* 2014. Contribution of above- and below-ground plant traits to the structure
695 and function of grassland soil microbial communities. *Annals of Botany* 114: 1011–1021.

696 Legendre P, Borcard D, Roberts DW. 2012. Variation partitioning involving orthogonal spatial
697 eigenfunction submodels. *Ecology* 93: 1234–1240.

698 Legendre P, Gallagher ED. 2001. Ecologically meaningful transformations for ordination of
699 species data. *Oecologia* 129: 271–280.

700 Legendre P, Legendre LFJ. 2012. *Numerical ecology*. Amsterdam, the Netherlands: Elsevier.

701 López-Angulo J, Pescador DS, Sánchez AM, Mihoč MAK, Cavieres LA, Escudero A. 2018.
702 Determinants of high mountain plant diversity in the Chilean Andes: From regional to local
703 spatial scales. *PLoS ONE* 13: 1–16.

704 Lynd LR, Paul J. Weimer, Zyl WH van, Pretorius IS. 2002. Microbial cellulose utilization:

fundamentals and biotechnology. *Microbiology and Molecular Biology Reviews* **66**: 506–577.

Maestre FT, Bowker MA, Puche MD, Hinojosa BM, Martínez I, García-Palacios P, Castillo AP, Soliveres S, Luzuriaga AL, Sánchez AM, *et al.* 2009. Shrub encroachment can reverse desertification in semi-arid Mediterranean grasslands. *Ecology Letters* **12**: 930–941.

Matesanz S, Pescador DS, Pías B, Sánchez AM, Chacón-Labella J, Illuminati A, de la Cruz M, López-Angulo J, Marí-Mena N, Vizcaíno A, *et al.* 2019. Estimating belowground plant abundance with DNA metabarcoding. *Molecular Ecology Resources* **19**: 1265– 1277.

Millard P, Singh BK. 2010. Does grassland vegetation drive soil microbial diversity? *Nutrient Cycling in Agroecosystems* **88**: 147–158.

Mokany K, Raison RJ, Prokushkin AS. 2006. Critical analysis of root:shoot ratios in terrestrial biomes. *Global Change Biology* **12**: 84–96.

Orwin KH, Buckland SM, Johnson D, Turner BL, Smart S, Oakley S, Bardgett RD. 2010. Linkages of plant traits to soil properties and the functioning of temperate grassland. *Journal of Ecology* **98**: 1074–1083.

Peralta AML, Sánchez AM, Luzuriaga AL, de Bello F, Escudero A. 2019. Evidence of functional species sorting by rainfall and biotic interactions: A community monolith experimental approach. *Journal of Ecology* **107**: 2772–2788.

Pescador DS, de la Cruz M, Chacón-Labella J, Pavón-García J, Escudero A. 2020. Tales from the underground: Soil heterogeneity and not only above-ground plant interactions explain fine-scale species patterns in a Mediterranean dwarf-shrubland. *Journal of Vegetation Science* **31**: 497–508.

Pescador DS, Sánchez AM, Luzuriaga AL, Sierra-Almeida A, Escudero A. 2018. Winter is coming: plant freezing resistance as a key functional trait for the assembly of annual Mediterranean communities. *Annals of botany* **121**: 335–344.

Philippot L, Raaijmakers JM, Lemanceau P, Van Der Putten WH. 2013. Going back to the roots: The microbial ecology of the rhizosphere. *Nature Reviews Microbiology* **11**: 789–799.

Prober SM, Leff JW, Bates ST, Borer ET, Firn J, Harpole WS, Lind EM, Seabloom EW, Adler PB, Bakker JD, *et al.* 2015. Plant diversity predicts beta but not alpha diversity of soil microbes across grasslands worldwide. *Ecology Letters* **18**: 85–95.

Reintal M, Tali K, Haldna M, Kull T. 2010. Habitat preferences as related to the prolonged dormancy of perennial herbs and ferns. *Plant Ecology* **210**: 111–123.

Rousk J, Bååth E, Brookes PC, Lauber CL, Lozupone C, Caporaso JG, Knight R, Fierer N. 2010. Soil bacterial and fungal communities across a pH gradient in an arable soil. *ISME Journal* **4**: 1340–1351.

Schenk HJ, Jackson RB. 2002. Rooting depths, lateral root spreads and below-ground/above-ground allometries of plants in water-limited ecosystems. *Journal of Ecology* **90**: 480–494.

Serna-Chavez HM, Fierer N, Van Bodegom PM. 2013. Global drivers and patterns of microbial abundance in soil. *Global Ecology and Biogeography* **22**: 1162–1172.

Shi S, Richardson AE, O'Callaghan M, Deangelis KM, Jones EE, Stewart A, Firestone MK, Condron LM. 2011. Effects of selected root exudate components on soil bacterial communities. *FEMS Microbiology Ecology* **77**: 600–610.

Silver WL, Miya RK. 2001. Global patterns in root decomposition: Comparisons of climate and litter quality effects. *Oecologia* **129**: 407–419.

Soil Survey Staff. 2014. *Keys to soil taxonomy*. Blacksburg, VA, USA: Pocahontas Press.

Stegen JC, Lin X, Fredrickson JK, Konopka AE. 2015. Estimating and mapping ecological processes influencing microbial community assembly. *Frontiers in Microbiology* **6**: 1–15.

Stegen JC, Lin X, Konopka AE, Fredrickson JK. 2012. Stochastic and deterministic assembly processes in subsurface microbial communities. *ISME Journal* **6**: 1653–1664.

Tabatabai MA. 1982. Soil enzymes. In: Page AL, Miller RH, Keeney DR, eds. *Methods of soil analysis*. Madison, Wisconsin, USA: American Society of Agronomy and Soil Science Society of America, 501–538.

Tedersoo L, Bahram M, Dickie IA. 2014. Does host plant richness explain diversity of ectomycorrhizal fungi? Re-evaluation of Gao et al. (2013) data sets reveals sampling effects. *Molecular Ecology* **23**: 992–995.

Tedersoo L, Mett M, Ishida TA, Bahram M. 2013. Phylogenetic relationships among host plants explain differences in fungal species richness and community composition in ectomycorrhizal symbiosis. *New Phytologist* **199**: 822–831.

Träger S, Öpik M, Vasar M, Wilson SD. 2019. Belowground plant parts are crucial for comprehensively estimating total plant richness in herbaceous and woody habitats. *Ecology* **100**: 1–12.

Trinder CJ, Johnson D, Artz RRE. 2009. Litter type, but not plant cover, regulates initial litter

767 decomposition and fungal community structure in a recolonising cutover peatland. *Soil Biology*
768 *and Biochemistry* **41**: 651–655.

769 **Tuomela M, Vikman M, Hatakka A, Itävaara M. 2000**. Biodegradation of lignin in a compost
770 environment: A review. *Bioresource Technology* **72**: 169–183.

771 **Uroz S, Buée M, Murat C, Frey-Klett P, Martin F. 2010**. Pyrosequencing reveals a contrasted
772 bacterial diversity between oak rhizosphere and surrounding soil. *Environmental Microbiology*
773 *Reports* **2**: 281–288.

774 **Vandenkoornhuyse P, Mahé S, Ineson P, Staddon P, Ostle N, Cliquet JB, Francez AJ, Fitter AH,**
775 **Young JPW. 2007**. Active root-inhabiting microbes identified by rapid incorporation of plant-
776 derived carbon into RNA. *Proceedings of the National Academy of Sciences of the United States*
777 *of America* **104**: 16970–16975.

778 **Vos M, Wolf AB, Jennings SJ, Kowalchuk GA. 2013**. Micro-scale determinants of bacterial
779 diversity in soil. *FEMS Microbiology Reviews* **37**: 936–954.

780 **de Vries FT, Hoffland E, van Eekeren N, Brussaard L, Bloem J. 2006**. Fungal/bacterial ratios in
781 grasslands with contrasting nitrogen management. *Soil Biology and Biochemistry* **38**: 2092–
782 2103.

783 **de Vries FT, Manning P, Tallowin JRB, Mortimer SR, Pilgrim ES, Harrison KA, Hobbs PJ, Quirk H,**
784 **Shipley B, Cornelissen JHC, *et al.* 2012**. Abiotic drivers and plant traits explain landscape-scale
785 patterns in soil microbial communities. *Ecology Letters* **15**: 1230–1239.

786 **Waldrop MP, Zak DR, Blackwood CB, Curtis CD, Tilman D. 2006**. Resource availability controls
787 fungal diversity across a plant diversity gradient. *Ecology Letters* **9**: 1127–1135.

788 **Wardle DA. 2006**. The influence of biotic interactions on soil biodiversity. *Ecology Letters* **9**: 870–
789 886.

790 **Wardle DA, Bardgett RD, Klironomos JN, Setälä H, Van Der Putten WH, Wall DH. 2004**. Ecological
791 linkages between aboveground and belowground biota. *Science* **304**: 1629–1633.

792 **Wardle DA, Yeates GW. 1993**. The dual importance of competition and predation as regulatory
793 forces in terrestrial ecosystems: evidence from decomposer food-webs. *Oecologia* **93**: 303–306.

794 **Wubs ERJ, Bezemer TM. 2016**. Effects of spatial plant-soil feedback heterogeneity on plant
795 performance in monocultures. *Journal of Ecology* **104**: 364–376.

796 **Yang P, van Elsas JD. 2018**. Mechanisms and ecological implications of the movement of bacteria
797 in soil. *Applied Soil Ecology* **129**: 112–120.

798 Zhou J. 2017. Stochastic Community Assembly: Does It Matter in Microbial Ecology?
799 *Microbiology and Molecular Biology Reviews* 81: 1–32.

800 Zuur AF, Ieno EN, Elphick CS. 2010. A protocol for data exploration to avoid common statistical
801 problems. *Methods in Ecology and Evolution* 1: 3–14.

802

803 *Supporting Information*

804 Methods S1 Bioinformatic analyses to assess microbial diversity.

805 Methods S2 R packages used for specific applications.

806 Table S1 Summary statistics for soil physicochemical variables from the study area.

807 Table S2 Loadings of each soil physicochemical variable on the four PCA axes after a varimax
808 rotation.

809 Table S3 Results of the AICc-based model selection applied to each set of predictors for
810 microbial richness based on Poisson generalized linear models.

811 Table S4 Results of the AICc-based model selection based on final Poisson generalized linear
812 models testing the response of bacterial and fungal richness to all set of predictors.

813 Table S5 Correlations (Pearson coefficient) among the predictors.

814 Table S6 Relative abundance (based on sequence reads) of bacterial taxa at taxonomic level of
815 family, order, class and phylum, across 83 soil samples.

816 Table S7 Relative abundance (based on sequence reads) of fungal taxa at taxonomic level of
817 family, order, class and phylum, across 83 soil samples.

818 Table S8 Partial Mantel tests of the relationship between the microbial β-diversity and the
819 dissimilarities in below- and aboveground plant composition, soil properties, and spatial
820 covariates.

821 Fig. S1 Sampling design.

822 Fig. S2 Rarefaction curves of bacterial and fungal communities for each soil-microbial sample.

823 Fig. S3 Diagram showing the sampling of the aboveground plant community.

824 Fig. S4 Non-metric multidimensional scaling (nMDS) ordinations showing patterns of variation in
825 below- and aboveground plant composition.

826 Fig. S5 Relationship between below- and aboveground plant community attributes.

827 **Fig. S6** Relative abundance (based on sequence reads) of bacteria and fungi at the phyla
828 taxonomic level.

Fig. 1. Venn diagrams showing variance partitioning results of microbial richness (number of OTUs), species composition and β-diversity (based on Bray–Curtis distance) of the bacterial and fungal communities explained by the four sets of predictors: belowground plant community attributes (Roots), aboveground plant community attributes (Above-), soil properties (Soil) and spatial covariates (Space). The variables of each set of predictors which were included in the variance partitioning analysis were selected using a model selection procedure based on the sum of Akaike weights (see table S3 for the model selections). The reported values are adjusted R^2, representing the unique and shared variance explained by each predictor. Areas and intersections without values represent 0% explained and 0% shared variance, respectively.

Fig. 2. Regression lines showing the response of bacterial (taupe) and fungal (blue) richness (number of OTUs) to the belowground and aboveground plant community attributes. The solid and dashed lines indicate significant and no significant effects, respectively.

Fig. 3. Relationships between the β-diversity of soil bacterial and fungal communities among samples and the β-diversity of belowground and aboveground plant communities (based on Bray-Curtis distance). Residuals from partial multivariate correlograms are represented to statistically control for the effects of the β-diversity of the opposite component (aboveground or belowground), the soil physicochemical properties and spatial covariates (based on Euclidean distance). The solid and dashed lines, respectively, indicate significant and not significant relationships using partial Mantel tests. *rho* is the Spearman's correlation determined via partial Mantel tests and *p* is the reached probability level (permutations 999).

Fig. 4. Conceptual diagram summarizing the main results of the study. Responses of species richness, composition and β-diversity of bacterial and fungal communities to root biomass, composition, and β-diversity. (a) Root biomass positively affected fungal richness. (b) Root composition affected both bacterial composition and richness. (c) Bacterial β-diversity was significantly correlated with root β-diversity. The significance of these relationships was tested after removing the effect of the aboveground plant component, soil physicochemical properties and other spatially structured variables.

Table 1. Results of model selection based on Poisson GLMs testing the response of bacterial and fungal richness. Standardized coefficient estimates (mean), associated 2.5% and 97.5% confidence intervals (CI) and variance inflation factor (VIF). Predictors with 95% CI excluding zero are shown in bold. Abbreviations: Root comp.1, belowground plant composition based on the axis 1 of an non-metric multidimensional scaling (nMDS; Fig. S4a); Root comp.2, belowground plant composition based on the axis 2 of an nMDS (Fig. S4a); Aboveground comp.2, aboveground community composition based on the axis 2 of an nMDS (Fig. S4b); dbMEM9 and dbMEM29, distance-based Moran's eigenvectors maps reflecting broad and fine spatial structures, respectively; X and Y, X and Y coordinates, respectively.

Bacteria				
Predictor	Estimate	2.5% CI	97.5% CI	VIF
(Intercept)	5.358	5.345	5.37	
Aboveground richness	0	-0.01	0.020	1.97
Aboveground comp.2	0.002	-0.004	0.023	1.199
Root comp.2	**0.017**	**0.004**	**0.030**	**1.476**
Fertility	**0.022**	**0.009**	**0.034**	**1.367**
Salinity	0.003	-0.002	0.023	2.372
dbMEM9	0.009	0.001	0.027	1.167

Fungi				
Predictor	Estimate	2.5% CI	97.5% CI	VIF
(Intercept)	4.418	4.394	4.442	
Root biomass	**0.037**	**0.013**	**0.061**	**1.933**
Root comp.1	0	-0.007	0.006	2.381
Root comp.2	0.015	-0.015	0.046	1.509
Aboveground richness	-0.004	-0.025	0.016	1.973
Plant cover	0.020	-0.011	0.051	1.513
Aboveground comp.2	**-0.039**	**-0.064**	**-0.013**	**1.194**
Fertility	**-0.034**	**-0.060**	**-0.009**	**1.274**
Salinity	-0.003	-0.018	0.013	1.350
Soil carbon	-0.002	-0.015	0.011	1.847
dbMEM29	**0.051**	**0.026**	**0.075**	**1.180**

X	0.001	-0.010	0.012	2.743
Y	0.001	-0.008	0.009	2.956

865 **Table 2.** ANOVA-like results based on partial RDAs testing the effect of the forward-selected
866 below- and aboveground plant attributes, soil variables and spatial covariates on the bacterial
867 and fungal composition. The effect of individual predictors of each set was tested after
868 controlling for the effects of the remaining three sets of predictors. The *F-ratio-like* statistic was
869 tested using the Monte Carlo test based on 999 permutations. ***$p < 0.001$, ** $p < 0.01$, * $p <$
870 0.05.
871

Predictor set / Predictor	Bacteria			Fungi		
	Monte Carlo test			Monte Carlo test		
	F-ratio	*p*		F-ratio	*p*	
Belowground plant attributes						
Root biomass				1.05	0.356	
Composition 1	1.40	0.019	*	1.26	0.088	
Aboveground plant attributes						
Composition 1	0.92	0.693		1.39	0.040	*
Soil properties						
Carbon	1.62	0.007	**	0.93	0.617	
Texture	1.38	0.034	*	1.07	0.314	
Salinity	0.94	0.599		1.24	0.097	
Spatial covariates						
x	2.59	0.001	***	2.37	0.001	***
y	2.32	0.001	***	3.07	0.001	***
MEM2	1.58	0.009	**	3.07	0.001	***
MEM4				1.58	0.013	*
MEM5				1.37	0.036	*
MEM6				1.73	0.006	**
MEM7				2.03	0.001	***
MEM8	1.32	0.049		1.36	0.040	*
MEM9				1.37	0.052	.
MEM10				1.58	0.006	**
MEM12	1.18	0.117				
MEM29	1.94	0.003	**	1.68	0.009	**

872

New Phytologist Supporting Information

Article title: The role of root community attributes in predicting soil fungal and bacterial community patterns

Authors: Jesús López-Angulo, Marcelino de la Cruz, Julia Chacón-Labella, Angela Illuminati, Silvia Matesanz, David S. Pescador, Beatriz Pías, Ana M. Sánchez and Adrián Escudero

Article acceptance date: 04 June 2020

The following Supporting Information is available for this article:

Methods S1 Bioinformatic analyses to assess microbial diversity

DNA was isolated using the DNeasy PowerSoil isolation kit (Qiagen, CA, USA) from 0.25 g of dry soil from the 83 soil samples, following the manufacturer's instructions, and resuspended in a final volume of 100 µL. Extraction blanks were included in every DNA extraction round to check for cross-contamination. For library preparation, a fragment of the bacterial 16S rRNA (≈460 bp) (PCR conditions: 95 ºC for 5 min; 25 cycles at 95 ºC for 0.5 min, 50 ºC for 0.5 min and 72 ºC for 0.5 min; and 72 ºC for 10 min), and the complete fungal ITS2 region (≈300 bp) (PCR conditions: 95 ºC for 5 min; 35 cycles at 95 ºC for 0.5 min, 49 ºC for 0.5 min and 72 ºC for 0.5 min; and 72 ºC for 10 min) were amplified. 16S rRNA gene was amplified using the primers Bakt 341F (5′- CCT ACG GGN GGC WGC AG-3′) and Bakt 805R (5′- GAC TAC HVG GGT ATC TAA TCC -3′) (Herlemann *et al.* 2011) and the ITS2 gene using the primers ITS86F (5′- GTG AAT CAT CGA ATC TTT GAA -3′) (Turenne *et al.* 1999) and ITS4 (5′- TCC TCC GCT TAT TGA TAT GC -3′) (White *et al.* 1990) to which the Illumina sequencing primer sequences were attached at their 5' ends. PCRs were carried out in a final volume of 25 µL, containing 1-2.5 µL of template DNA, 0.5 µM of the primers, 12.5 µL of Supreme NZYTaq 2x Green Master Mix (NZYTech, Lisbon, Portugal), and ultrapure water up to 25 µL. The reaction mixture was incubated with an initial denaturation at 95ºC for 5 min, followed by 25-35 cycles of 95ºC for 30'', 47-50ºC for 30'', 72ºC for 30'', and a final extension step at 72ºC for 10'. A second PCR per sample and group with 5 cycles and 60ºC as annealing temperature was performed to attach the index sequences required for multiplexing different libraries in the same sequencing pool. Negative controls with no DNA were included to check for contamination during library preparation. Libraries were run on 2% agarose gels stained with GreenSafe (NZYTech, Lisbon, Portugal), viewed under UV light to verify library size and purified using the Mag-Bind RXNPure Plus magnetic beads (Omega Biotek, Norcross, GA, USA). Libraries were then pooled in equimolar amounts according to the quantification data provided by the Qubit dsDNA HS Assay

Kit (Thermo Fisher Scientific, Waltham, MA, USA). The pool was sequenced in a MiSeq PE300 run (Illumina).

The quality of the Illumina paired-end raw FASTQ files [consisting of forward (R1) and reverse (R2) reads] was checked using FastQC (Andrews 2010). Paired-end assembly of the R1 and R2 reads was performed with FLASH (Magoč & Salzberg 2011). The mismatch resolution in the overlapping region (minimum overlap of 30 base pairs) was accomplished by keeping the base with the higher quality score. CUTADAPT 1.3 (Martin 2011) was used to remove sequences that did not contain the PCR primers (allowing up to 2 mismatches) and those shorter than 300 or 400 nucleotides (for bacteria and fungi, respectively). Sequences were quality-filtered (minimum Phred quality score of 20) and labelled using the *multiple_split_libraries.py* script implemented in Qiime (Caporaso *et al.* 2010). A label was added to the headers of the FASTQ file in order to identify each sample when sequences are combined to perform downstream analysis.

The FASTA files were processed using the VSEARCH bioinformatic tool (Rognes *et al.* 2016). It has been shown that reference-based clustering methods may greatly overestimate OTU diversity (Edgar 2018a) compared to *de novo* clustering (Westcott & Schloss 2015; Porter & Hajibabaei 2018). Furthermore, a recent study has challenged the widely-used 97% threshold for 16S ribosomal RNA OTUs (Edgar 2018b). Therefore, we used *de novo* OTU clustering, increasing the similarity threshold. Sequences were dereplicated (-derep fulllength), clustered at a similarity threshold of 100 % (-cluster fast, {centroids option), and sorted (-sortbysize). Artifacts (such as point mutations and chimeras) that may be generated during PCR and sequencing were filtered during the bioinformatic pipeline. *De novo* chimera detection was carried out using the UCHIME algorithm (Edgar *et al.* 2011) implemented in VSEARCH.

The taxonomic assignment of the bacterial OTUs was performed by querying the clustered centroids against the SILVA reference database (Quast *et al.* 2012; Qiime release 132) using the script *assign_taxonomy.py* implemented in Qiime and the UCLUST algorithm (Edgar 2010) with a 97 % similarity threshold. For fungi, we used the UNITE reference database (UNITE Community 2017: UNITE QIIME release Version 01.12.2017. https://doi.org/10.15156/BIO/587481), using the same script as above and the BLAST algorithm (Altschul *et al.* 1990) with a maximum E-value of $1e^{-9}$ and a minimum percent identity of 90 %. An OTU table with the number of sequences of each OTU in each sample was created for each group.

A quality-filtering was applied to the OTU tables to remove the OTUs occurring at a frequency below 0.005 % in the whole dataset (Bokulich *et al.* 2013). In DNA metabarcoding

studies it has been observed that a low percentage of the reads of a library can be assigned to another library. This phenomenon, referred to as mistagging, tag jumping, index hopping, index jumping, etc. is the result of the miss-assignment of the indices during library preparation, sequencing, and/or demultiplexing steps (Esling, Lejzerowicz & Pawlowski 2015; Bartram *et al.* 2016). In order to correct for this phenomenon, the low abundance OTUs of each sample (0.1 % threshold) were removed. Finally, only the OTUs that matched sequences in the reference databases at the specified of 99 % were maintained in the OTU tables. The unidentified OTUs were removed from the OTU table for downstream analysis. For fungi, despite the suitability of the primers used to specifically amplify the ITS2 region of Fungi, sequences belonging to Plantae and other unidentified Eukaryota were clustered during the OTU picking process. These OTUs were also removed from the fungi OTU table for downstream analyses.

References

Altschul, S.F., Gish, W., Miller, W., Myers, E.W. & Lipman, D.J. 1990. Basic local alignment search tool. *Journal of Molecular Biology,* **215,** 403-410.

Andrews, S. 2010. FastQC: a quality control tool for high throughput sequence data.

Bartram, J., Mountjoy, E., Brooks, T., Hancock, J., Williamson, H., Wright, G., Moppett, J., Goulden, N. & Hubank, M. 2016. Accurate sample assignment in a multiplexed, ultrasensitive, high-throughput sequencing assay for minimal residual disease. *The Journal of Molecular Diagnostics,* **18,** 494-506.

Bokulich, N.A., Subramanian, S., Faith, J.J., Gevers, D., Gordon, J.I., Knight, R., Mills, D.A. & Caporaso, J.G. 2013. Quality-filtering vastly improves diversity estimates from Illumina amplicon sequencing. *Nature Methods,* **10,** 57.

Caporaso, J.G., Kuczynski, J., Stombaugh, J., Bittinger, K., Bushman, F.D., Costello, E.K., Fierer, N., Pena, A.G., Goodrich, J.K. & Gordon, J.I. 2010. QIIME allows analysis of high-throughput community sequencing data. *Nature Methods,* **7,** 335.

Edgar, R.C. 2010. Search and clustering orders of magnitude faster than BLAST. *Bioinformatics,* **26,** 2460-2461.

Edgar, R.C. 2018a. Accuracy of taxonomy prediction for 16S rRNA and fungal ITS sequences. *PeerJ,* **6,** e4652.

Edgar, R.C. 2018b. Updating the 97% identity threshold for 16S ribosomal RNA OTUs. *Bioinformatics,* **34,** 2371-2375.

Edgar, R.C., Haas, B.J., Clemente, J.C., Quince, C. & Knight, R. 2011. UCHIME improves sensitivity and speed of chimera detection. *Bioinformatics,* **27,** 2194-2200.

Esling, P., Lejzerowicz, F. & Pawlowski, J. 2015. Accurate multiplexing and filtering for high-throughput amplicon-sequencing. *Nucleic Acids Research,* **43,** 2513-2524.

Magoč, T. & Salzberg, S.L. 2011. FLASH: fast length adjustment of short reads to improve genome assemblies. *Bioinformatics,* **27,** 2957-2963.

Martin, M. 2011. Cutadapt removes adapter sequences from high-throughput sequencing reads. *EMBnet. journal,* **17,** pp. 10-12.

Morgan, B.S. & Egerton-Warburton, L.M. 2017. Barcoded NS31/AML2 primers for sequencing of arbuscular mycorrhizal communities in environmental samples. *Applications in plant sciences,* **5,** 1700017.

Porter, T.M. & Hajibabaei, M. 2018. Scaling up: A guide to high-throughput genomic approaches for biodiversity analysis. *Molecular Ecology,* **27,** 313-338.

Quast, C., Pruesse, E., Yilmaz, P., Gerken, J., Schweer, T., Yarza, P., Peplies, J. & Glöckner, F.O. 2012. The SILVA ribosomal RNA gene database project: improved data processing and web-based tools. *Nucleic Acids Research,* **41,** D590-D596.

Rognes, T., Flouri, T., Nichols, B., Quince, C. & Mahé, F. 2016. VSEARCH: a versatile open source tool for metagenomics. *PeerJ,* **4,** e2584.

Turenne CY, Sanche SE, Hoban DJ, Karlowsky JA, Kabani AM. 1999. Rapid identification of fungi by using the ITS2 genetic region and an automated fluorescent capillary electrophoresis system. *Journal of clinical microbiology* **37**: 1846–1851.

White TJ, Bruns T, Lee S, Taylor J. 1990. Amplification and direct sequencing of fungal ribosomal RNA genes for phylogenetics. In: Innis M, Gelfand D, Sninsky J, White T, eds. PCR protocols: a guide to methods and applications. Academic Press San Diego, CA, 315–322.

Westcott, S.L. & Schloss, P.D. 2015. De novo clustering methods outperform reference-based methods for assigning 16S rRNA gene sequences to operational taxonomic units. *PeerJ,* **3,** e1487.

Methods S2 R packages used for specific applications.

Bacterial and fungal reads were rarefied using the function 'Rarefy' in 'GUniFrac' R package (Chen *et al.*, 2012). We used several functions from the 'vegan' R package (Oksanen *et al.*, 2010): the rarefaction curves were estimated using the function 'rarecurve'; the dissimilarity matrices and the non-metric multidimensional scaling (nMDS) ordinations were respectively computed with functions 'vegdist' and 'metaMDS'; variance partitioning was computed using function 'varpart'; partial redundancy analyses (pRDA) and distance-based redundancy analyses (dbRDAs) were respectively computed with functions 'rda' and 'dbrda'. Computation of the dbMEM eigenvectors and forward selection were performed using 'dbmem' and 'forward.sel' functions from the 'adespatial' R package (Dray *et al.*, 2016). We checked for multi-collinearity between the predictors using the variance inflation factor (VIF). In all cases, VIFs values were smaller than 4 suggesting the absence of collinearity problems (Zuur *et al.*, 2010). VIFs were computed using the 'vif' function in 'car' R package (Fox & Weisberg, 2011). GLMs were fitted using the 'glm' function of the 'stats' R package. Model selection procedure and the evaluation of the importance were performed using the functions 'dredge' and 'importance' from the R package 'MuMIn' (Bartoń, 2013). The partial Mantel tests were performed using the 'mantel' function in 'ecodist' R package (Goslee & Urban 2007).

References

Bartoń K. 2013. *MuMIn: Multi-Model Inference*. R package version 1.43.17. [WWWdocument] URL https://cran.r-project.org/web/packages/MuMIn/ [accessed 1 June 2020].

Chen J, Bittinger K, Charlson ES, Hoffmann C, Lewis J, Wu GD, Collman RG, Bushman FD, Li H. 2012. Associating microbiome composition with environmental covariates using generalized UniFrac distances. *Bioinformatics* **28**: 2106–2113.

Dray S, Blanchet G, Borcard D, Guenard G, Jombart T, Larocque G, Legendre P, Madi N, Wagner HH. 2016. *Adespatial: multivariate multiscale spatial analysis.* R package version 0.3-8. [WWWdocument] URL https://cran.r-project.org/web/packages/adespatial/ [accessed 1 June 2020].

Fox J, Weisberg S. 2011. *An R companion to applied regression*. Thousand Oaks, CA, USA.

Goslee SC, Urban DL. 2007. The ecodist package for dissimilarity-based analysis of ecological data. *Journal of Statistical Software* **22**: 1–19.

Oksanen J, Blanchet FG, Kindt R, Legendre P, O'hara RB, Simpson GL, Solymos P, Stevens MHH, Wagner H. 2010. *Vegan: community ecology package*. R package version 2.5-6. [WWWdocument] URL https://cran.r-project.org/web/packages/vegan/ [accessed 1 June 2020].

Zuur AF, Ieno EN, Elphick CS. 2010. A protocol for data exploration to avoid common statistical problems. *Methods in Ecology and Evolution* **1**: 3–14.

Table S1 Summary statistics for soil physicochemical variables from the study area. Mean, standard deviation (SD), minimum (min) and maximum (max) values, and coefficient of variation (CV) of 11 soil physicochemical variables for the 83 soil samples. Abbreviations: Gluc, β-glucosidase (µmol/gr dry soil/h); Phos, acid phosphatase activity (µmol/gr dry soil/h); SOC, soil organic carbon (%); N, soil total nitrogen (mg/g soil); P, soil available phosphorus (mg/g soil); K, potassium content (mg/g soil); Cond, electric conductivity (µS/cm).

Statistic	Gluc (µmol/gr/h)	Phos (µmol/gr/h)	SOC (%)	N (mg/g)	P (mg/g)	K (mg/g)	pH -	Cond (µS/cm)	Sand (%)	Silt (%)	Clay (%)
Mean	0.74	0.52	1.21	0.65	0.11	0.01	8.19	84.26	39.91	49.05	11.04
SD	0.41	0.24	0.30	0.27	0.04	0.00	0.12	29.80	3.36	2.22	1.96
Min	0.09	0.16	0.65	0.06	0.00	0.01	7.70	40.60	30.70	44.42	7.82
Max	2.26	1.40	2.29	1.51	0.21	0.02	8.41	198.30	46.40	55.01	17.49
CV	0.55	0.45	0.25	0.42	0.39	0.27	0.01	0.35	0.08	0.05	0.18

Table S2 Loadings of each soil physicochemical variable on the four PCA axes after a varimax rotation. PCA components represent variation in soil organic carbon (PC1), soil texture (PC2), fertility (PC3) and salinity (PC4). The proportion of variance of the soil physicochemical variables explained by each axis is provided (%). Abbreviations: Gluc and Phos, activity of β-glucosidase and phosphatase, SOC, soil organic carbon; N, soil total nitrogen; P, soil total phosphorus; K, available potassium; pH, soil pH; Cond, electric conductivity; Sand, Silt and Clay, percentage of sand, silt and clay.

Soil variable	PC1	PC2	PC3	PC4
SOC	0.77	-0.05	0.18	0.28
Gluc	0.78	-0.25	-0.12	0.13
Phos	0.84	0.09	0.01	0.01
N	0.3	-0.03	0.06	0.93
P	0.06	-0.01	-0.09	0.97
K	-0.02	0	0.54	-0.05
pH	-0.16	0.06	-0.86	-0.11
Cond	-0.08	0.31	0.79	-0.06
Sand	0.08	-0.99	-0.08	0.02
Silt	-0.2	0.78	0	-0.12
Clay	0.11	0.82	0.1	0.09
Proportion of variance (%)	19	22	16	18
Cumulative Proportion of variance (%)	19	53	69	87

Table S3 Results of the AICc-based model selection applied to each set of predictors for microbial richness based on Poisson generalized linear models. Corrected Akaike Information Criterion (AICc) and delta of the best selected models for bacterial (a-d) and fungal (e-h) richness. The predictors selected by their importance relative (wi > 0.4) are shown in bold. Poisson generalized linear models (GLMs) were fitted one for each of the four sets of predictors: belowground (a and e) and aboveground (b and f) plant component, soil properties (c and g) and space (d and h). Variance inflation factor (VIF) of the predictors are also shown.

a)

glm (bacterial richness ~ root predictor set, family=Poisson)						
Belowground component	models				w_i	VIF
(Intercept)	5.357	5.357	5.358	5.357		
Root biomass				0.005	0.20	1.05
Root richness		-0.006			0.18	1.65
Root composition1					0.00	1.58
Root composition2	0.015	0.016		0.014	**0.81**	1.05
AICc	664.11	665.63	665.79	665.90		
delta	0.00	1.52	1.68	1.79		
weight	0.43	0.20	0.19	0.18		

b)

glm bacterial richness ~ Aboveground predictor set, family=Poisson						
Aboveground component	models				w_i	VIF
(Intercept)	5.358	5.358	5.358	5.358		
Aboveground biomass					0.00	1.31
Aboveground richness			0.003		0.20	1.45
Aboveground composition1		-0.004			0.20	1.13
Aboveground composition2				0.003	0.00	1.02
AICc	673.30	675.11	675.22	675.23		
delta	0.00	1.80	1.91	1.93		
weight	0.46	0.19	0.18	0.18		

c)

glm (bacterial richness ~ soil predictor set, family=Poisson)						
Soil	models				w_i	VIF
(Intercept)	5.357	5.357	5.357	5.357		
Carbon			-0.007	-0.007	0.33	1.00
Texture						1.00
Fertility	0.012		0.012		**0.56**	1.00
Salinity	0.020	0.020	0.020	0.020	**1.00**	1.00

AICc	660.44	660.91	661.86	662.29
delta	0.00	0.47	1.42	1.85
weight	0.37	0.30	0.18	0.15

d)

glm (bacterial richness ~ spatial predictor set, family=Poisson)

Space	models			w_i	VIF
(Intercept)	5.357	5.358	5.357		
MEM9	-0.014		-0.014	**0.71**	1.03
X				0.00	1.03
Y			0.004	0.20	1.00
AICc	664.64	665.79	666.56		
delta	0.00	1.15	1.91		
weight	0.51	0.29	0.20		

e)

glm (fungal richness ~ root predictor set, family=Poisson)

Belowground component	models	w_i	VIF
(Intercept)	4.421		
Root biomass	0.037	**1.00**	1.05
Root richness		0.00	1.65
Root composition1		0.00	1.57
Root composition2	0.043	**1.00**	1.05
AICc	795.20		
delta	0.00		
weight	1.00		

f)

glm fungal richness ~ Aboveground predictor set, family=Poisson

Aboveground component	models				w_i	VIF
(Intercept)	4.421	4.421	4.421	4.421		
Aboveground biomass	0.038	0.036	0.044	0.044	**1.00**	1.31
Aboveground richness			-0.013	-0.019	0.37	1.45
Aboveground composition1		0.013		0.018	**1.00**	1.12
Aboveground composition2	-0.044	-0.043	-0.043	-0.042	0.40	1.02
AICc	798.48	799.62	799.84	800.23		
delta	0.00	1.14	1.36	1.75		
weight	0.40	0.23	0.20	0.17		

g)

glm (fungal richness ~ soil predictor set, family=Poisson)

Soil	models						w_i	VIF
(Intercept)	4.422	4.422	4.421	4.422	4.421	4.421		
Carbon				-0.012		-0.0123	0.26	1.00
Texture			0.013		0.0127		0.27	1.00
Fertility		-0.017			-0.0165	-0.0166	**0.46**	1.00
Salinity	-0.036	-0.036	-0.036	-0.036	-0.036	-0.036	**1.00**	1.00
AICc	808.20	808.50	809.30	809.40	809.7	809.7		
delta	0.00	0.29	1.05	1.13	1.42	1.46		
weight	0.25	0.22	0.15	0.14	0.123	0.12		

h)

glm (fungal richness ~ spatial predictor set, family=Poisson)

Space	models	w_i	VIF
(Intercept)	4.420		
dbMEM29	0.060	**1.00**	1.02
X	0.031	**1.00**	1.02
Y		0.00	1.00
AICc	784.20		
delta	0.00		
weight	1.00		

Table S4 Results of the AICc-based model selection based on final Poisson generalized linear models testing the response of bacterial (a) and fungal (b) richness to all set of predictors. Standardized regression coefficients of the model predictors and its variance inflation factor (VIF). Only models which differed from the best model in less than 2 AICc units are shown. Abbreviations: dbMEM9 and dbMEM29, distance-based Moran's eigenvectors maps reflecting broad and fine spatial structures, respectively; X and Y, X and Y coordinates. Corrected Akaike Information Criterion (AICc) and delta of the best selected models (AICc < 2) for bacterial (a) and fungal (b)..

Results of model selection based on Poisson GLMs testing the response of bacterial and fungal richness.

a)

glm (bacterial richness ~ Aboveground richness + Plant cover + Aboveground comp.1 + Aboveground comp.2 + Root richness + Root biomass + Root comp.1 + Root comp.2 + Soil carbono + Texture + Fertility + Salinity + dbMEM29 + X + Y, family=Poisson)								
	models							VIF
(Intercept)	5.358	5.358	5.357	5.358	5.357	5.357	5.358	
Aboveground richness							0.006	
Aboveground composition2				0.008	0.011			1.269
Root composition2	0.017	0.016	0.017	0.019	0.019	0.016	0.017	1.478
Fertility		0.010				0.010		1.262
Texture	0.021	0.021	0.022	0.022	0.023	0.021	0.021	1.352
dbMEM29	0.014	0.014		0.012			0.015	1.209
AICc	657.219	657.673	658.238	658.457	658.499	658.529	658.956	
delta	0.000	0.454	1.019	1.238	1.280	1.310	1.737	
weight	0.227	0.181	0.136	0.122	0.120	0.118	0.095	

b)

glm (fungal richness ~ Aboveground richness + Plant cover + Aboveground comp.1 + Aboveground comp.2 + Root richness + Root biomass + Root comp.1 + Root comp.2 + Soil carbono + Texture + Fertility + Salinity + dbMEM29 + X + Y, family=Poisson)

	models														VIF
(Intercept)	4.418	4.418	4.418	4.418	4.418	4.418	4.418	4.418	4.418	4.418	4.418	4.418	4.418	4.418	
Aboveground richness		-0.020				-0.019						-0.021			1.973
Plant cover	0.021	0.031		0.023	0.026	0.033	0.023	0.021		0.023	0.023	0.030	0.023		1.513
Aboveground composition1															1.771
Aboveground composition2	-0.039	-0.037	-0.036	-0.043	-0.042	-0.041	-0.039	-0.037	-0.035	-0.037	-0.039	-0.035	-0.039	-0.041	1.194
Root richness															1.933
Root biomass	0.035	0.036	0.037	0.037	0.039	0.037	0.037	0.035	0.037	0.039	0.037	0.036	0.036	0.039	1.459
Root composition1													-0.010		2.381
Root composition2	0.022	0.022	0.025					0.025	0.027	0.023	0.019	0.025	0.023		1.509
Soil carbono					-0.017						-0.012				1.847
Texture															2.490
Fertility								-0.014	-0.015			-0.015			1.274
Salinity	-0.033	-0.031	-0.038	-0.035	-0.035	-0.033	-0.030	-0.033	-0.038	-0.034	-0.033	-0.031	-0.034	-0.040	1.350
dbMEM29	0.049	0.051	0.050	0.052	0.052	0.055	0.051	0.048	0.049	0.049	0.049	0.050	0.049	0.054	1.180
X							0.017								2.743
Y										0.013					2.956
AICc	765.856	766.370	766.370	766.483	766.976	766.992	767.093	767.141	767.400	767.436	767.501	767.543	767.703	767.748	
delta	0.000	0.513	0.514	0.626	1.120	1.136	1.236	1.285	1.543	1.579	1.644	1.686	1.847	1.891	
weight	0.124	0.096	0.096	0.091	0.071	0.070	0.067	0.065	0.057	0.056	0.055	0.053	0.049	0.048	

Table S5 Correlations (Pearson coefficient) among the predictors. Red, blue, green and orange denote variables related to roots, aboveground, soil physicochemical properties and spatial covariables, respectively. Abbreviations are: RR, root richness; RB, root mass; RC1, Root composition.1; RC2, Root composition.2; CR, Aboveground richness; CB, Aboveground cover; CC1, Aboveground composition.1; CC2, Aboveground composition.2; PCA1, PCA axis 1; PCA2, PCA axis 2; PCA3, PCA axis 3; PCA4, PCA axis 4; x, coordinate x; Y, coordinate y; MEM29, MEM9, MEM11, spatial eigenvectors representing variables with different spatial scale.

	RR	RB	RC1	RC2	CR	CB	CC1	CC2	PCA1	PCA2	PCA3	PCA4	X	Y	MEM29	MEM9	MEM11
RR	1	-0.13	0.59	0.20	0.16	0.39	0.27	-0.09	0.13	0.13	-0.18	-0.10	0.15	-0.18	0.02	0.18	0.09
RB		1	0.05	0.08	0.07	0.11	0.33	0.02	0.14	0.16	-0.01	0.10	-0.03	-0.34	0.11	-0.03	0.19
RC1			1	0.10	0.22	0.45	0.51	0.01	0.03	0.30	-0.03	-0.11	0.28	-0.42	-0.04	0.15	0.19
RC2				1	0.11	0.06	0.06	-0.19	-0.28	0.22	0.12	-0.09	0.45	-0.07	0.20	-0.11	-0.04
CR					1	0.49	0.15	0.10	0.16	0.25	-0.05	-0.23	0.04	-0.23	0.08	-0.06	0.26
CB						1	0.33	0.11	0.30	0.22	-0.07	-0.03	-0.12	-0.37	0.11	0.12	0.20
CC1							1	0.00	0.05	0.35	-0.11	-0.16	0.19	-0.46	-0.04	0.19	0.04
CC2								1	0.10	-0.06	0.10	-0.10	-0.19	-0.20	-0.09	-0.09	0.08
PCA1									1	0.01	0.00	-0.01	-0.46	-0.04	-0.01	0.17	-0.02
PCA2										1	-0.01	0.01	0.30	-0.59	-0.11	-0.30	-0.02
PCA3											1	0.00	0.15	-0.09	-0.07	-0.07	-0.13
PCA4												1	-0.25	0.08	-0.09	-0.23	0.06
X													1	0.02	0.10	-0.01	-0.15
Y														1	0.01	0.17	-0.34
MEM29															1	0.00	0.00
MEM9																1	0.00
MEM11																	1

Table S6 Relative abundance (based on sequence reads) of bacterial taxa at taxonomic level of family, order, class and phylum, across 83 soil samples

Phylum		Class		Order		Family	
Acidobacteria	0.23	Acidobacteria	0.06	Acidobacteriales	0.01	Acidobacteriacea(Subgrou1)	0.02
				Solibacterales	0.21	Solibacteracea(Subgrou3)	0.41
		Blastocatelli(Subgrou4)	0.54	Blastocatellales	0.13	Blastocatellaceae	0.26
				Pyrinomonadales	1.77	Pyrinomonadaceae	3.47
		Subgrou6	0.04	unculture Acidobacteribacterium	0.08	unculture Acidobacteribacterium	0.17
		Thermoanaerobaculia	0.08	Thermoanaerobaculales	0.29	Thermoanaerobaculaceae	0.56
Actinobacteria	2.79	0319-7L14	0.04	unculture actinobacterium	0.10	unculture actinobacterium	0.19
		Acidimicrobiia	0.50	IMCC26256	0.46	unculture Acidimicrobidabacterium	0.00
				Microtrichales	1.08	Ilumatobacteraceae	0.58
		Actinobacteria	1.13	Corynebacteriales	0.10	Mycobacteriaceae	0.20
				Frankiales	0.88	Frankiaceae	0.14
						Geodermatophilaceae	1.36
						Nakamurellaceae	0.13
						Sporichthyaceae	0.02
				Micrococcales	0.97	Intrasporangiaceae	0.04
						Microbacteriaceae	0.30
						Micrococcaceae	1.25
						Promicromonosporaceae	0.31
				Micromonosporales	0.53	Micromonosporaceae	1.04
				Propionibacteriales	0.47	Nocardioidaceae	0.74
						Propionibacteriaceae	0.18
				Pseudonocardiales	0.64	Pseudonocardiaceae	1.26
				Streptomycetales	0.40	Streptomycetaceae	0.78
				Streptosporangiales	0.00	Thermomonosporaceae	0.01
		Rubrobacteria	1.45	Rubrobacterales	5.13	Rubrobacteriaceae	10.05
		Thermoleophilia	5.29	Gaiellales	13.04	Gaiellaceae	4.24
						uncultured	25.50
				Solirubrobacterales	5.58	67-14	9.86
						Solirubrobacteraceae	1.04
Armatimonadetes	0.00	Fimbriimonadia	0.00	Fimbriimonadales	0.00	Fimbriimonadaceae	0.01
Bacteroidetes	0.02	Bacteroidia	0.06	Chitinophagales	0.16	Chitinophagaceae	0.32
				Cytophagales	0.06	Hymenobacteraceae	0.09
						Microscillaceae	0.03
Chloroflexi	0.32	Anaerolineae	0.01	Anaerolineales	0.02	Anaerolineaceae	0.04
				SBR1031	0.00	A4b	0.01
		Chloroflexia	0.21	Kallotenuales	0.00	AKIW781	0.00
				Thermomicrobiales	0.75	JG30-KF-CM45	1.48
		Dehalococcoidia	0.01	S085	0.03	metagenome	0.00

		KD4-96	0.36	unculture bacterium	3.69	unculture bacterium	8.68
				unculture	0.15	unculture	0.30
				Chloroflexbacterium		Chloroflexbacterium	
		Ktedonobacteria	0.01	C0119	0.00	unculture soibacterium	0.01
				Ktedonobacterales	0.04	Ktedonobacteraceae	0.09
Cyanobacteria	0.01	Oxyphotobacteria	0.02	Nostocales	0.07	Phormidiaceae	0.14
Firmicutes	0.00	Bacilli	0.00	Bacillales	0.01	Bacillaceae	0.02
Gemmatimonadetes	0.11	Gemmatimonadetes	0.32	Gemmatimonadales	1.14	Gemmatimonadaceae	2.24
		Longimicrobia	0.02	Longimicrobiales	0.06	Longimicrobiaceae	0.12
Planctomycetes	0.01	Phycisphaerae	0.02	Tepidisphaerales	0.07	WD210soigroup	0.14
		Planctomycetacia	0.00	Gemmatales	0.01	Gemmataceae	0.01
				Isosphaerales	0.00	Isosphaeraceae	0.00
Proteobacteria	1.08	Alphaproteobacteria	2.88	Acetobacterales	0.01	Acetobacteraceae	0.02
				Azospirillales	0.03	Azospirillaceae	0.03
						Inquilinaceae	0.01
				Caulobacterales	0.21	Caulobacteraceae	0.41
				Dongiales	0.16	Dongiaceae	0.32
				Puniceispirillales	0.08	PuniceispirillaleIncertaSedis	0.16
				Reyranellales	0.02	Reyranellaceae	0.04
				Rhizobiales	3.09	Beijerinckiaceae	1.81
						Devosiaceae	0.01
						Hyphomicrobiaceae	0.01
						Labraceae	0.04
						Rhizobiaceae	0.54
						RhizobialeIncertaSedis	0.14
						Rhodomicrobiaceae	0.01
						Xanthobacteraceae	1.08
				Rhodobacterales	0.05	Rhodobacteraceae	0.10
				Sphingomonadales	6.46	Sphingomonadaceae	12.67
				Tistrellales	0.00	Geminicoccaceae	0.00
		Deltaproteobacteria	0.11	Myxococcales	0.27	Archangiaceae	0.03
						bacteriap25	0.50
						Sandaracinaceae	0.00
		Gammaproteobacteria	0.44	Betaproteobacteriales	1.20	Burkholderiaceae	1.63
						Nitrosomonadaceae	0.64
						TRA3-20	0.09
				Enterobacteriales	0.12	Enterobacteriaceae	0.24
				Nitrosococcales	0.23	Nitrosococcaceae	0.45
				Oceanospirillales	0.00	Pseudohongiellaceae	0.00
				Steroidobacterales	0.01	Steroidobacteraceae	0.01
				Xanthomonadales	0.00	Xanthomonadaceae	0.00
Verrucomicrobia	0.05	Verrucomicrobiae	0.16	Chthoniobacterales	0.57	Chthoniobacteraceae	1.11
				Opitutales	0.00	Opitutaceae	0.00
				Pedosphaerales	0.00	Pedosphaeraceae	0.01

Table S7 Relative abundance (based on sequence reads) of fungal taxa at taxonomic level of family, order, class and phylum, across 83 soil samples

Phylum		Class		Order		Family	
Ascomycota	76.47	Archaeorhizomycetes	0.25	Archaeorhizomycetales	0.37	Archaeorhizomycetaceae	0.00
		Dothideomycetes	8.56	Botryosphaeriales	0.07	Botryosphaeriaceae	0.00
				Capnodiales	0.03	Cladosporiaceae	0.00
						Mycosphaerellaceae	0.00
						Teratosphaeriaceae	0.00
				Dothideales	0.01	Aureobasidiaceae	0.00
				Pleosporales	2.61	Cucurbitariaceae	0.00
						Dictyosporiaceae	0.00
						Didymellaceae	0.00
						Didymosphaeriaceae	0.00
						Lentitheciaceae	0.00
						Leptosphaeriaceae	0.00
						Phaeosphaeriaceae	0.00
						Pleosporaceae	0.00
						Sporormiaceae	0.00
				Tubeufiales	0.19	Tubeufiaceae	0.00
		Eurotiomycetes	16.90	Chaetothyriales	2.09	Herpotrichiellaceae	0.02
						Trichomeriaceae	0.00
				Eurotiales	0.24	Aspergillaceae	0.00
				Onygenales	0.99	Gymnoascaceae	0.00
						Onygenaceae	0.01
						OnygenalefaIncertasedis	0.00
				Phaeomoniellales	0.01	Phaeomoniellaceae	0.00
				unidentified	36.98	unidentified	0.42
				Verrucariales	0.30	Verrucariaceae	0.00
		Geoglossomycetes	0.01	Geoglossales	0.02	Geoglossaceae	0.00
		Lecanoromycetes	1.85	Caliciales	0.02	Physciaceae	0.00
				Lecanorales	1.98	Lecanoraceae	0.00
						Parmeliaceae	0.02
						Ramalinaceae	0.00
				Lecideales	0.05	Lecideaceae	0.00
				Teloschistales	0.04	Teloschistaceae	0.00
				Umbilicariales	0.01	Umbilicariaceae	0.00
		Leotiomycetes	1.08	Helotiales	1.52	Dermateaceae	0.00
						HelotialefaIncertasedis	0.01
				Thelebolales	0.05	Thelebolaceae	0.00
		Orbiliomycetes	0.15	Orbiliales	0.21	Orbiliaceae	0.00
		Pezizomycetes	19.20	Pezizales	27.93	Ascobolaceae	0.00
		Pezizomycetes	19.20			Helvellaceae	0.01
						Pezizaceae	0.03
						Pyronemataceae	0.15
						Tuberaceae	0.09
		Sordariomycetes	1.97	Diaporthales	0.01	Valsaceae	0.00
				Hypocreales	0.84	Cordycipitaceae	0.00
						HypocrealefaIncertasedis	0.00
						Nectriaceae	0.00
						Stachybotryaceae	0.00

						Tilachlidiaceae	0.00
				Sordariales	0.24	Chaetomiaceae	0.00
						Lasiosphaeriaceae	0.00
				Xylariales	0.29	Microdochiaceae	0.00
						Sporocadaceae	0.00
						Xylariaceae	0.00
Basidiomycota	22.14	Agaricomycetes	14.79	Agaricales	4.66	Clavariaceae	0.00
		Agaricomycetes	14.79			Entolomataceae	0.00
						Hygrophoraceae	0.00
						Inocybaceae	0.04
						Psathyrellaceae	0.00
						Stephanosporaceae	0.00
						Tricholomataceae	0.00
				Boletales	0.03	Boletaceae	0.00
						Melanogastraceae	0.00
				Cantharellales	0.50	Ceratobasidiaceae	0.01
				Polyporales	0.01	Meruliaceae	0.00
				Sebacinales	3.72	Sebacinaceae	0.04
						Serendipitaceae	0.00
				Thelephorales	12.17	Thelephoraceae	0.12
		Geminibasidiomycetes	0.01	Geminibasidiales	0.02	Geminibasidiaceae	0.00
		Tremellomycetes	0.32	Filobasidiales	0.43	Piskurozymaceae	0.00
Chytridiomycota	0.11	Rhizophlyctidomycetes	0.00	Rhizophlyctidales	0.00	Rhizophlyctidaceae	0.00
		Spizellomycetes	0.05	Spizellomycetales	0.08	Spizellomycetaceae	0.00
Mortierellomycota	1.28	Mortierellomycetes	0.88	Mortierellales	1.28	Mortierellaceae	0.01

Table S8 Partial Mantel tests of the relationship between the microbial β-diversity and the dissimilarities in below- and aboveground plant composition, soil properties, and spatial covariates. *rho* is the Spearman's rho statistic. Significant values (<0.05) are shown in bold.

	Bacteria		Fungi	
Predictors	*rho*	*p*	*rho*	*P*
Belowground plant	**0.13**	**0.024**	0.09	0.114
Aboveground plant	0.06	0.124	**0.12**	**0.009**
Soil properties	**0.18**	**0.004**	0.11	0.053
Spatial covariates	**0.22**	**<0.001**	**0.37**	**<0.001**

Fig. S1 Sampling design. It consisted of 64 sampling units (blue circles) on an 8 × 8 m regular grid system. In addition, another 20 sampling units (dark purple triangles) were established to assess a finer spatial scale.

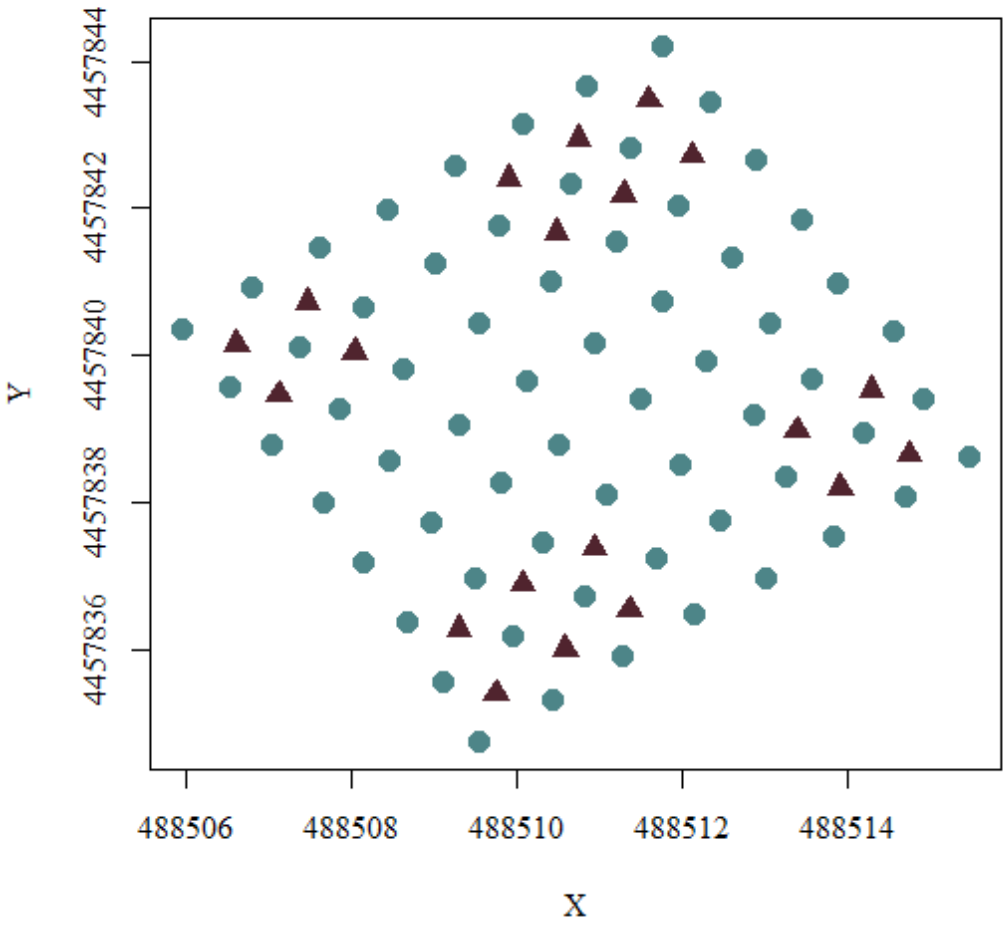

Fig. S2 Rarefaction curves of bacterial (taupe) and fungal (blue) communities for each soil-microbial sample.

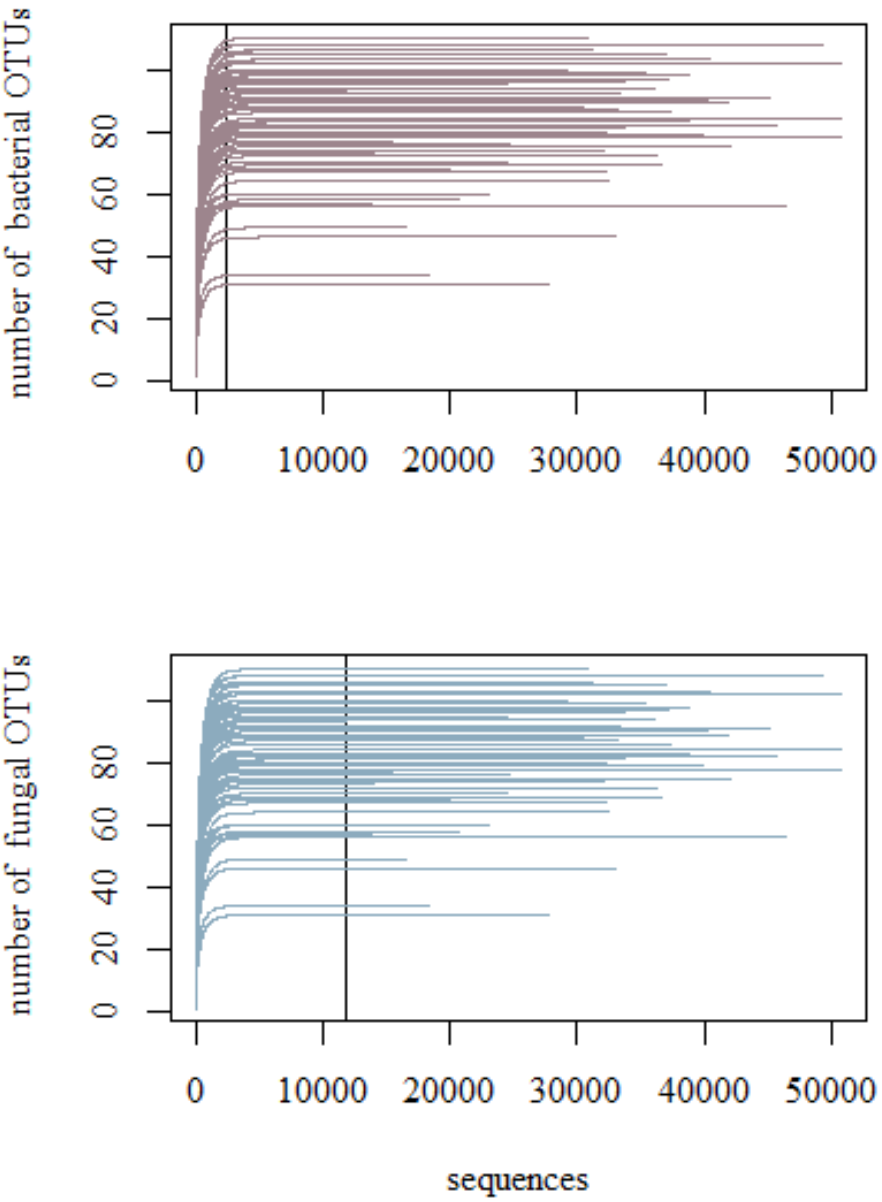

Fig. S3 Diagram showing the sampling of the aboveground plant community. The green circles represent the projection of the crown of each individual plant in the 8 m × 8 m plot. The brown circles represent the intersection areas between the projection of the crown of each individual plant and a sampling circle of 20 cm radius around each sampling point

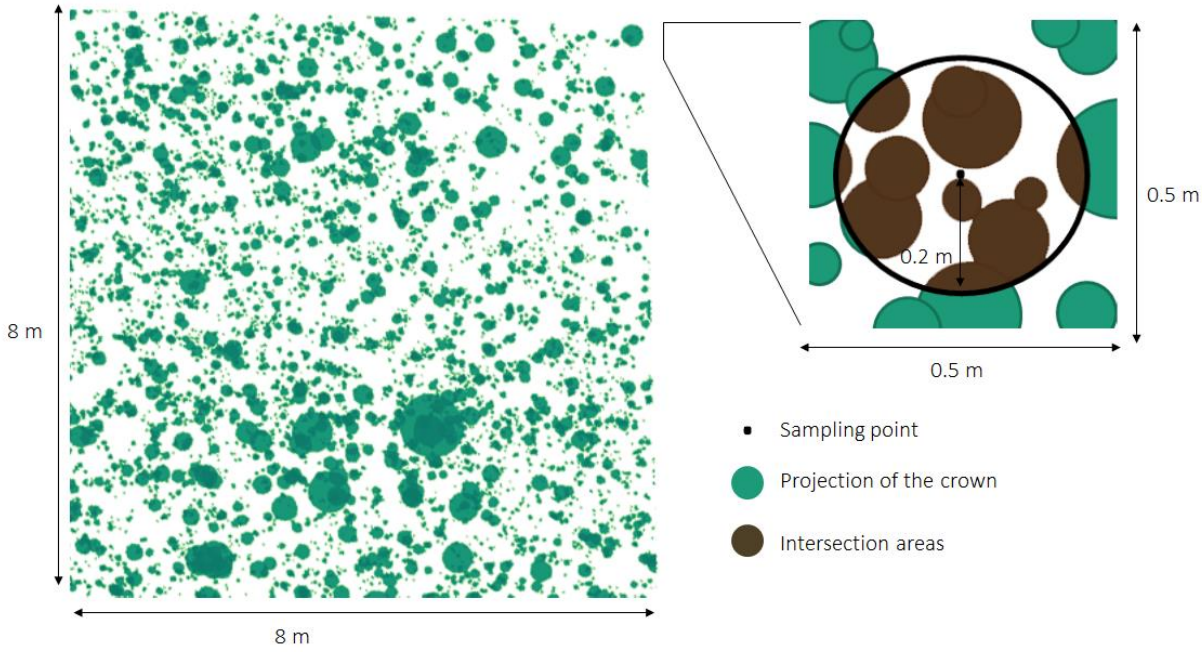

Fig. S4 Non-metric multidimensional scaling (nMDS) ordinations showing patterns of variation in (a) belowground and (b) aboveground plant composition based on 83 sample units.

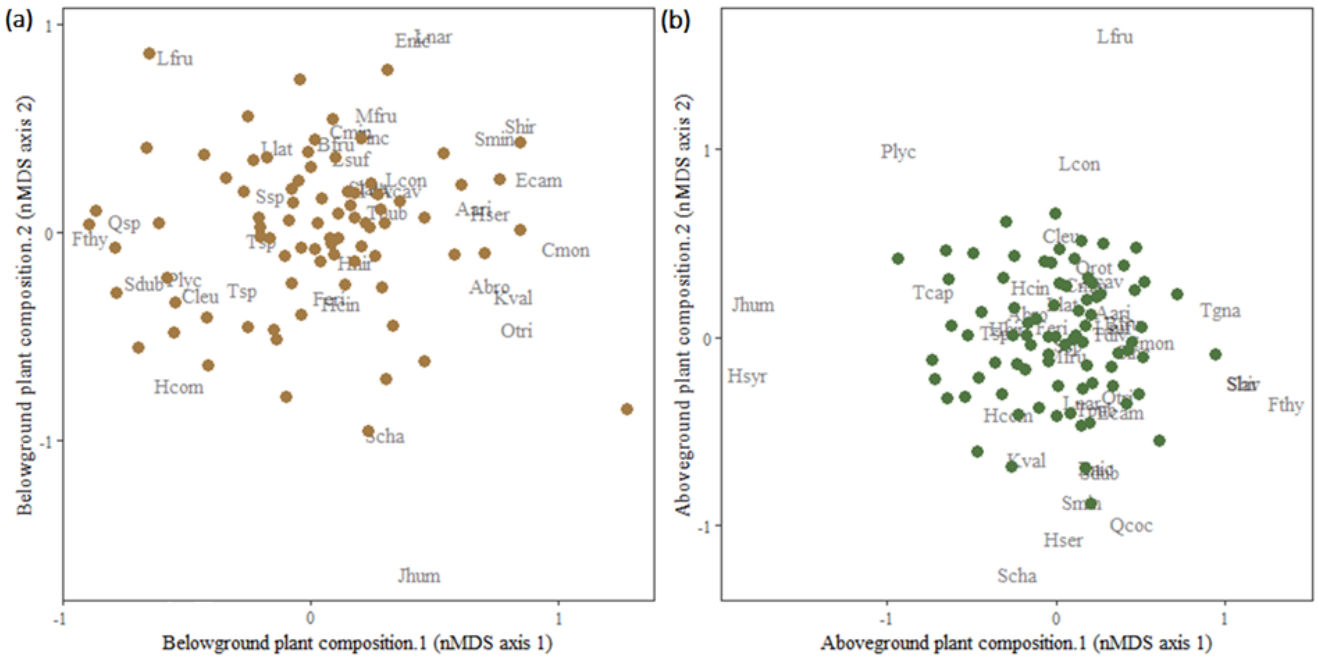

Abbreviations: Acav, Arenaria cavanillesiana; Apau, Aristolochia paucinervis; Aari, Asperula aristata; Ainc, Astragalus incanus; Abro, Avenula bromoides; Bfru, Bupleurum fruticescens; Chys, Centaurea hyssopifolia; Cleu, Cephalaria leucantha; Cmon, Coris monspeliensis; Cmin, Coronilla minima; Ecam, Eryngium campestre; Enic, Euphorbia nicaeensis; Feri, Fumana ericoides; Fthy, Fumana thymifolia; Hcin, Helianthemum cinereum; Hhir, Helianthemum hirtum; Hsyr, Helianthemum syriacum; Hser, Helychrisum serotinum; Hcom, Hippocrepis commutata; Jhum, Jurinea humilis; Kval, Koeleria vallesiana; Llat, Lavandula latifolia; Lcon, Leuzea conifera; Lnar, Linum narbonense; Lsuf, Linum suffruticosum; Lfru, Lithodora fruticosa; Mfru, Matthiola fruticulosa; Otri, Ononis tridentata; Plyc, Phlomis lychinitis; Qcoc, Quercus coccifera; Qrot, Quercus rotundifolia; Slav, Salvia lavandulifolia; Smin, Sanguisorba minor; Scha, Santolina chamaecyparissus; Shir, Sideritis hirsuta; Sinc, Sideritis incana; Sdub, Staehelina dubia; Ssp, Stipa sp; Tcap, Teucrium capitatum; Tgna, Teucrium gnaphalodes; Tdiv, Thesium divaricatum; Tpub, Thymelaea pubescens; Tsp, Thymus sp.

Fig. S5 Relationship between below- and aboveground plant community attributes. (a) Relationship between below- and aboveground plant richness. (b) Relationship between root biomass and aboveground plant cover. (c) Non-metric multi-dimensional scaling (nMDS) ordination showing patterns of variation in belowground and aboveground plant community composition among 83 soil samples.

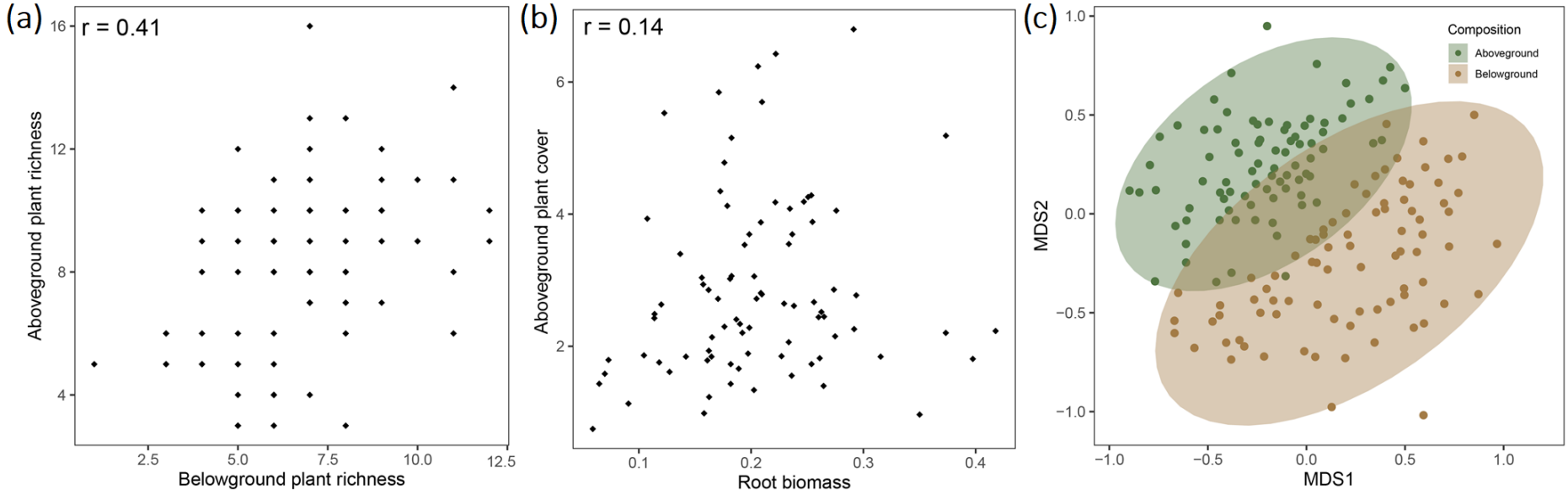

Fig. S6 Relative abundance (based on sequence reads) of bacteria and fungi at the phyla taxonomic level across 83 soil samples